

# Urban Aerosols and Their Variations with Clouds and Rainfall: A Case Study for New York and Houston

MENGLIN JIN,<sup>1</sup> J. MARSHALL SHEPHERD,<sup>2</sup> AND MICHAEL D. KING<sup>3</sup>

Short title: Urban Aerosols and Their Variations with Clouds and Rainfall

*Journal of Geophysical Research*  
(Manuscript revised August 2004)

---

<sup>1</sup> Department of Meteorology, University of Maryland, College Park, Maryland.

<sup>2</sup> Laboratory for Atmospheres, NASA Goddard Space Flight Center, Greenbelt, Maryland.

<sup>3</sup> Earth Sciences Directorate, NASA Goddard Space Flight Center, Greenbelt, Maryland.

**Authors** □ Dr. Menglin Jin  
Department of Meteorology  
University of Maryland  
College Park, MD 20742  
(301) 405-8833  
(301) 314-9482 (fax)  
mjin@atmos.umd.edu

Dr. J. Marshall Shepherd  
NASA Goddard Space Flight Center  
Code 912  
Greenbelt, MD 20771  
(301) 614-6327

Dr. Michael D. King  
NASA Goddard Space Flight Center  
Code 900  
Greenbelt, MD 20771  
(301) 614-5636

## Abstract

Diurnal, weekly, seasonal, and interannual variations of urban aerosols were analyzed with an emphasis on summer months using 4-years of the National Aeronautics and Space Administration (NASA) Earth Observing System (EOS) Moderate Resolution Imaging Spectroradiometer (MODIS) observations, *in situ* Aerosol RObotic NETwork (AERONET) observations, and *in situ* EPA PM<sub>2.5</sub> data for one mid-latitude city (New York) and one sub-tropical city (Houston). Seasonality is evident in aerosol optical thickness measurements, with a minimum in January and a maximum in April to July. The diurnal variations of aerosols, however, are detectable but largely affected by local and regional weather conditions, such as surface and upper-level winds. On calm clear days, aerosols peak during the two rush hours in the morning and evening. Furthermore, the anthropogenic-induced weekly cycles of aerosols and clouds are analyzed, which by themselves are weak as the anthropogenic signal is mixed with noises of natural weather systems. In addition, corresponding cloud properties observed from MODIS demonstrate an opposite phase to the seasonality of aerosols. No clear relationship observed between monthly mean aerosols and rainfall measurements from NASA's Tropical Rainfall Measuring Mission (TRMM), suggesting that the aerosol impact is not the primary reason for the change of rainfall amount. These analyses suggest spatial and temporal aerosol variations are important in order to fully simulate urban environment in a climate model.

## 1. Introduction

The most recent Intergovernmental Panel on Climate Change report (IPCC 2001) confirms that “there is new and stronger evidence showing that most of the warming observed over the last 50 years is attributed to human activities.” Although IPCC has an emphasis on greenhouse warming, urban-induced surface warming (“urban heat island effect”, UHI) and urban pollution impacts on surface energy budget have raised great concerns (Changnon 1992, Grindmond and Oke, 1995, Arnfield, 2003, IPCC 2001, Jin et. al. 2004, Shepherd and Jin 2004). Urban areas, with rapid land cover and land use changes, suffer significantly from human activities. Understanding the human impacts on nature is a central component of global change studies. And simulating urban environments in a climate model framework is the practical research approach (Jin et al. 1997).

Aerosols and their relationships with clouds and rainfall are one of the weakest aspects of current climate modeling [Ghan et. al. 2001, Collings, personal communication 2003]. Two limitations exist in the current urban modeling: one is that the aerosol effects on land surface skin temperature<sup>4</sup> (namely, UHI) is either not included or unrealistically represented; and another is that cloud-aerosol-rainfall relationships are not fully understood. Previous results, via different approaches, were controversial. For example, some studies reported that urban areas reduce rainfall due to cloud microphysics (Rosenfeld, 2000; Rathananthen et al. 2001), while other studies showed that urban areas significantly

---

<sup>4</sup> Land surface skin temperature is the radiometric temperature retrieved from satellite remote sensing based on the Planck function. This variable is a counterpart of the traditional WMO station measured 2m surface air temperature, but is more close to the surface energy balance. It has been used to study global climate change. Atmosphere conditions such as clouds and aerosols have significant influences on skin temperature. (Jin and Dickinson 1999, 2000, 2002, Jin 2000, 2004)

enhanced the intensity of storms and increased downwind rainfall (Huff and Vogel 1978, Changnon 1978, Shepherd et. al. 2002).

Better quantitative understanding of the spatial and temporal aerosol properties is desired in order to include urban aerosol radiative forcing and aerosol-cloud interactions in a general circulation model (GCM). Furthermore, observed climatological relationships between aerosols, clouds, and rainfall are needed for validating the modeled patterns in urban areas. This paper aims to describe the temporal variations of aerosols and to identify monthly mean aerosol-cloud-rainfall relationships from various remote sensing and ground-based measurements. Specifically, diurnal, weekly, seasonal, and interannual variations of urban aerosols are examined using 4-years of aerosol, cloud, rainfall, and land cover (namely, normalized difference vegetation index, NDVI) measurements from satellites. To demonstrate the similarities and differences of urban aerosols in different climate regions, we emphasize one mid-latitude city (New York) and one sub-tropical city (Houston). In addition, the large-scale variables (wind and surface pressure) from the National Centers for Environmental Prediction (NCEP) reanalysis reveal how the atmospheric system controls the transport of urban aerosols.

Aerosol radiative forcing, the so-called “direct effect,” means that aerosols reduce surface insolation by scattering and absorbing solar radiation and reemitting longwave radiation back to the surface [Ramanathan et al., 2001]. In addition, aerosols affect the climate system through aerosol-cloud interactions, primarily in three ways: (i) aerosols reduce the cloud effective radius and increase the cloud optical thickness as cloud condensation nuclei (CCN) increase, viz., the “indirect effect” [Twomey, 1977; King et al., 1993]; (ii) aerosol heating changes atmosphere stability and thus the occurrence and evaporation of clouds (“semi-indirect effect”) [Hansen et al., 1997]; and (iii) clouds affect aerosol properties. For

example, it was reported that the cloud diurnal cycle affects aerosol forcing over the Indian Ocean Experiment up to  $1\text{-}2\text{ Wm}^{-2}$  (*Podgomy et al.* [2001], manuscript unpublished). Similarly, aerosol size distribution can be changed due to aerosol-cloud interactions [*Remer and Kaufman*, 1998].

Produced by combustion of fossil fuels from traffic or industrial processes and modified through chemical composition, decomposition, and transport, urban aerosols are directly related to human life and are gaining increasing attention [*IPCC*, 2001; *Lelieveld et al.*, 2001; *Ramanathan et al.*, 2001; *Kaufman et al.*, 2002]. Figure 1 shows the simulated aerosol-induced changes in surface insolation based on the AERONET-observed aerosol optical properties for New York on one day in September (September 1, 2001). The total reduction in insolation for this day is about  $20\text{ Wm}^{-2}$ , with the maximum reduction at  $0.55\text{ }\mu\text{m}$  between clean and polluted cases. The calculation uses the NASA Global Modeling and Assimilation Office's (GMAO's) GCM radiative transfer scheme [*Chou and Suarez*, 1999]. The model requires input of aerosol optical thickness, single scattering albedo, asymmetry factor, vertical aerosol distribution, and cloud cover. Obviously, these properties of urban aerosols, spatially or temporally, are required in aerosol impact studies.

Spectral aerosol optical thickness (AOT) represents the attenuation of sunlight by a column of aerosols at certain wavelengths, and has been used to assess aerosol condensation (*Kaufman et al.* 2002). Therefore, AOT is the key parameter for modeling the radiative effects of aerosols in atmosphere columns, and is determined by the MODIS remote sensing algorithm [*Kaufman et al.* 1997; *Chu et al.*, 2002, 2003]. In this paper, we study optical thickness of aerosols and clouds to reveal their relationships. Furthermore, urban aerosols enhance aerosol-cloud interaction, which is expected to be more significant during the summer months when large-scale dynamic impact is relatively weak in comparison

to winter. Therefore, we emphasize the summer seasons for years 2000 - 2004.

Scale is critical in urban studies, as urban features vary dramatically along both horizontal and temporal dimensions [Oke, 1982; Jin *et al.*, 2004]. We analyzed cloud-rainfall-aerosol relationships at monthly instead of daily scale, in particular, because we intended to identify the typical, climatological sense of aerosol properties and their effects on clouds and rainfall, and partly because the daily variations are more affected by white noise from surface and atmospheric conditions than the longer scales, and thus are not the major focus of this study.

There are two foci in this paper. One is urban aerosols' temporal variations (diurnal, weekly, seasonal, and interannual variations). Such knowledge is desired to accurately parameterize aerosol physical and chemical processes in a climate model. Another focus is the correlations among aerosols, clouds, and rainfall. Instead of studying cloud microphysics, we compared monthly variations to reveal the possibly existing climatological relationships of these variables. These observed features are very useful in validating model performance.

The second section describes the data sets used in this work. The third section presents the results, and is followed by social, land cover, and general circulation backgrounds for New York and Houston that may shed light on explaining the differences in the aerosol properties for these two cities. Final remarks are presented in Section 5.

## 2. Data Sets

*MODIS Aerosol and Cloud Products* - Terra/MODIS monitors the aerosol optical thickness over the globe from a 705 km polar-orbiting sun-synchronous orbit that descends from north to south, crossing the equator at 10:30 local time. The aerosol optical thickness ( $\tau_a$ ) over land is retrieved at 0.47, 0.56 and 0.65  $\mu\text{m}$  and at a 10 km spatial resolution using the algorithm described by *Kaufman et al.*

[1997]. The spectral dependence of the reflectance across the visible wavelengths is then used to obtain a rough estimate of the fine mode (radius  $< 0.6 \mu\text{m}$ ) fraction of the aerosol optical thickness at  $0.56 \mu\text{m}$ . The cloud optical thickness ( $\tau_c$ ) and effective radius ( $r_e$ ) are retrieved at 1 km spatial resolution using the algorithm described by *King et al.* [1992] and *Platnick et al.* [2003]. These variables, as well as all other atmospheric properties from MODIS, are aggregated at daily, eight-day, and monthly time intervals on a global  $1^\circ \times 1^\circ$  latitude-longitude grid. These Level-3 products contain simple statistics (mean, standard deviation, etc.) computed for each parameter, and also contain marginal density and joint probability density functions between selected parameters [*King et al.*, 2003].

MODIS aerosol and cloud properties have been validated by field experiments and intercomparisons with ground-based observations [*Chu et al.*, 2002; *Mace et al.*, 2004]. Monthly mean aerosol and cloud products from Terra between April 2000 and September 2003 are utilized in the present study. In addition, daily cloud products from June to September 2001 are used for analysis of the weekly cycle of summer time urban aerosols.

*EPA PM<sub>2.5</sub> data* – Because Terra/MODIS only provides daytime measurements of aerosol optical thickness at  $\sim 10:30$  AM local time for clear conditions, *in situ* EPA PM<sub>2.5</sub> measurements are used to monitor the diurnal variation of aerosol concentration in this work. PM<sub>2.5</sub> refers to particle mass of particles less than  $2.5 \mu\text{m}$  diameter that generally consists of mixed solid and liquid aerosols in air and which excludes dust. PM<sub>2.5</sub> therefore captures the “fine” mode particles that are  $\leq 2.5 \mu\text{m}$  in diameter.

*AERONET daily data* – AErosol RObotic NETwork (AERONET) provides ground-based aerosol monitoring and data archive at  $\sim 170$  locations worldwide. Data of spectral aerosol optical thickness, size distribution, single scattering albedo, and precipitable water in diverse aerosol regions provide globally-

distributed near real time observations of aerosols [Holben *et al.*, 1998]. Hourly and daily AERONET measurements of aerosol optical thickness are used to identify the diurnal and weekly cycles of aerosol. The data are quality-ensured and cloud-screened [Eck *et al.*, 1999; Smirnov *et al.*, 2000].

*TRMM Rainfall Data* – TRMM was launched in November 1997 as a joint U.S.-Japanese mission to advance the understanding of the global energy and water cycle by providing distributions of rainfall and latent heating over the global tropics [Simpson *et al.*, 1988; Shepherd *et al.*, 2002]. To extend TRMM data from 40°N-40°S, we use the 3B42 monthly, 1° x 1° rain rate and rain accumulation product (Adler *et al.* 2000). This product uses TRMM microwave imager data to adjust merged infrared precipitation and root-mean-square precipitation error estimates. It should be noted that the quality of Product 3B-42 is highly sensitive to the quality of the input infrared and microwave data. If the quality of the input data sources is less than anticipated, then the quality of product 3B-42 will be degraded. Nevertheless, these corresponding, multi-year rainfall products help establish the relationships between aerosols, clouds, and precipitation.

*NDVI data* – A 20-year NDVI data set derived from AVHRR channel 1 and channel 2 radiances is used to compare the vegetation/land cover changes in the New York and Houston regions. This data set is at 8 km and produced at a monthly resolution.

*NCEP reanalysis* – The National Centers for Environmental Prediction (NCEP) Reanalysis and National Center for Atmospheric Research (NCAR) 50-year reanalysis [Kistler *et al.*, 2001] is used to reproduce the surface temperature and surface wind. The monthly-averaged model output has a spatial resolution of 2.5° x 2.5°. The NCEP reanalysis, like any other GCM output, has uncertainties, but the overall geographical distribution is proven to be realistic, and therefore suitable for use in providing weather conditions for New York and Houston.

### 3. Results

#### 3.1 Diurnal Variation

Figure 2 shows the global distribution of aerosol optical thickness at  $0.56 \mu\text{m}$  over both land and ocean for January 2002, except for locations where the surface is too bright to be able to retrieve the aerosol loading (e.g., Sahara, Saudi Arabia, Greenland). Urban regions of North America, Europe, India, and East Asia have larger aerosol optical thicknesses than most of the inner continents, with the exception of biomass burning in Gabon and the Democratic Republic of the Congo, and dust outbreaks from the Sahara that are transported across the Atlantic. As a consequence, the radiative forcing of aerosols is expected to be larger over urban areas than the inner continents where urban aerosols are largely absent. The maximum  $\tau_a \sim 0.8$  occurs along the Ganges Valley of India, large portions of China, and the eastern USA. It should be emphasized that  $\tau_a$  arises from all types of aerosols, not just those of anthropogenic origins from urban areas alone.

Spatial values of  $\tau_a$  ( $0.56 \mu\text{m}$ ) change 10% for the New York region in three continuous summers. Values are above 0.5 in June 2000 and June 2002, but only around 0.4 in June 2001 (cf. Figure 3). Considering that the change is on monthly mean scale, it is significant. In contrast, little change occurs in aerosol loading for three consecutive June months in Houston. Further study, as we will discuss below, suggests such differences are partly a result of local weather and climate conditions, and the subsequent transport of aerosols.

Since a large portion of urban aerosols is attributed to anthropogenic activities, which have observed day and night differences, diurnal variation of aerosols is expected (Dickerson et. al. 2001, Smirnov et. al. 2002 ). Aerosol concentration is also affected by boundary layer stability, which is stable at night and active during daytime as a result of surface temperature increase (Stull 1988). Aerosol

loading at the surface in urban areas is typically the smallest from late night to early morning (3-6 AM) and increases to the first maximum of the day at ~10 AM and then slightly drops in the afternoon until the arrival of the 2<sup>nd</sup> maximum of the day at about ~8 am, as shown in Figure 4a. The peaks are likely caused by early morning and late afternoon car combustion resulting from the rush hours. However, on most days, the diurnal cycle is strongly modified by weather conditions and is thus less typical than the classic case illustrated in Figure 4a, as implied by the error bar on the figures. Figure 4b shows that the peak aerosol quality index<sup>1</sup> of Houston occurs around 10 PM EST and 21 PM EST, attains a value of only 0.12, which is smaller than the 0.18 of New York. In addition, July monthly mean Ozone at Houston has a similar diurnal pattern. Again, the large error bar suggests that the instantaneous aerosol loading may significantly differ from the monthly average. Therefore, a further look at daily variation will help illustrate the ranges and reasons for diurnal behavior of urban aerosols.

One-day measurements from AERONET for the Goddard Institute for Space Studies (GSFC) located in New York City (Figure 5b) show that on July 15, 2001, there was a sharp increase in spectral aerosol optical thickness, from 0.5 at noon to 0.8 at 3 PM UTC time for 1020nm wavelength. Corresponding 7-day back-trajectory analysis of AERONET ( Fig. 5a) reveals that the original aerosols are transported from northern Canada. These transported aerosols are likely products of the Canadian forest fires started over central Quebec during the pe-

---

<sup>1</sup> Air quality index (AQI) is calculated by converting the measured pollutant concentrations into index values to reporting daily air quality. U.S. Environmental Protection Agency (EPA) calculates the AQI for five major air pollutants: ground-level ozone, PM, carbon monoxide, sulfur dioxide, and nitrogen dioxide. The AQI runs from 0 to 500. The higher the AQI value, the greater the level of air pollution and the larger the health concern. (see EPA web for details [www.epa.gov/air/air\\_quality\\_monitoring/air\\_quality\\_index](http://www.epa.gov/air/air_quality_monitoring/air_quality_index))

riod 5-9 July 2002 (Colarco et. al. 2004), because at the 850mb and 950mb pressure levels, the parcels transported to New York City were originally around the Quebec fire locations five days earlier (Fig. 5a). The back trajectories were derived from the NASA GSFC trajectory model (Schoeberl and Sparling, 1995, Thompson et. al. 2002), which uses the wind information provided by the Center for Environmental Prediction Center (NCEP) and NCAR reanalysis (Kistler et. al. 2001).

However, day-to-day aerosol variation is significant: on calm, clear days such as July 2, 6, and 7, 2001 (not shown), the diurnal aerosol optical thickness is smooth and as low as 0.04. By contrast, aerosol optical thickness on July 3 and 5, 2001 was 0.6-0.8 in late morning and slightly increased in the late afternoon before the occurrence of clouds inhibited further measurements (not shown). Unlike the variations at other longer time scales, the diurnal variation of aerosols is strongly controlled by local weather conditions, such as wind, which enhances the aerosol transport.

### **3.2 Seasonal and interannual variations**

Pronounced seasonality with a minimum in winter and a maximum in April to early summer is observed in both New York City and Houston based on Terra/MODIS Level-3 data analysis for 3 years (cf. Figure 6). For Houston, the minimum monthly mean aerosol optical thickness is  $<0.2$  in the four continuous years from 2000 to 2003, although the occurrence time of the minimum differs slightly: December in 2000, December to January in 2001, and November to January in 2002. The maxima are above 0.4 with the extreme value as high as 0.52 in April 2000. The occurrence of the maxima in April or May is hypothesized to correspond to the peak time of annual biomass burning in Mexico (Duncan et. al. 2003). For New York, large-scale frontal or jet stream weather systems are typically active during this transitional season, transporting the biomass burning-

emitted aerosols from Canada to New York City and through turbulent planetary boundary layer (PBL) mixing to move the upper-altitude-transported aerosols to the surface. By contrast, the minimum  $\tau_a$  ( $0.56 \mu\text{m}$ ) in New York is 0.15, lower than that of Houston, and the maximum  $\tau_a$  is above 0.5, consistent with that of Houston. Note that New York's January 2001 has a peak aerosol optical thickness while other Januarys have low optical thickness. Further examination of the daily observations of AERONET and the NCEP reanalysis suggest that this peak in January 2001 may be an error in data analysis.

### 3.3 Weekly Variation

Previous research on urban pollutant transport revealed a weekday-weekend differences in ozone, nitrogen oxide and non-methane hydrocarbon in California (Marr and Harley 2002a, b), as a result of vehicle emission. Specifically, emissions of  $\text{NO}_x$  on weekends are about 30% less than on weekdays due to a large decrease of heavy-duty truck activity. As a result, higher  $\text{O}_3$  were observed during the weekend than on weekdays due to a series of chemical processes which produce  $\text{O}_3$  from  $\text{NO}_x$  (Dickerson et al. 1997). Such weekly variation has been called the "weekend effect" (Marr and Harley 2002b), which was originally reported in the 1970s (Lebron 1975) and has been detected in New York City, Los Angeles, St. Louis, Vancouver, San Francisco, and Switzerland (Cleveland et al. 1974, Lonneman et al. 1974, Elkus and Wilson 1977).

Research on rainfall over New York at surrounding oceanic regions also show larger weekend rainfall than weekdays (so-called "wet-Saturday", Cervený and Balling, 1998). Aerosols' weekly variations were attributed to such rainfall weekly differences (Cervený and Balling, 1998). Similarly, based on multi-year TRMM rainfall measurements, weekly cycle has been identified for many regions of Northern Hemisphere for summer time, although the weekly signal is so weak that it may not be detectable for one specific year (Bell, personal communication

2004).

To address if a weekday cycle in urban aerosols indeed exists and how strong this signal is, we examined the three continuous summers (2000, 2001, 2002) using the daily AERONET *in situ* measurements. Correspondingly, we use MODIS clouds properties to examine if the weekly cycle is resolvable in the clouds fields.

The weekly cycle of AOT over New York City as derived from AERONET observations (Fig. 7) shows high values during weekdays and low values on weekends. The peak appears on Wednesday. This is consistent with the previous urban aerosol reports (Marr and Harley, 2002a,b; Linacre and Geerts, 2002). Daily data for August-September 2000, June-September 2001, and June-September 2002 from AERONET GISS station have been sampled. Several average and filtering methods were tested to examine whether the weekly cycle signal is present. We notice that AOT over New York City can be 0.02 to 0.8, depending on surface traffic and overlying atmospheric winds. To reduce the high AOT transported from outside of the city, we only selected the days having AOT < 0.2. In addition, we only sampled the measurements taken during the evening because urban surface has warm anomalies than the surrounding regions (i.e., urban heat island effect, *Jin et al.*, 2004) and thus results in active convection in early afternoon. Consequently, the urban atmospheric column would be less stable than the surrounding areas, indicating a higher probability of the city-induced convective activities which disturb surface aerosol concentration [*Orville et al.*, 2001; *Shepherd et al.* 2002, *Shepherd and Burian*, 2003].

The signals of weekly variation are distinct from year to year (Fig. 8). Summer 2001 has a stronger signal with the overall AOT close or above 0.05 and the average Wednesday value above 0.1. By comparison, in 2000 and 2002 summers, the weekday-weekend differences are smaller. This suggests that the

weekly cycle is very weak and may not be valid for all years, but further study is warranted.

Correspondingly, a weekly cycle of cloud properties is also evident (Figure 9), with water cloud effective radius peaks on Wednesday and liquid water path peaks on weekends. The data are derived from daily Terra/MODIS level-2 cloud observations using the algorithm described by *Platnick et al.* [2003]. Again, these weekly cycles may be a result of human activities since no natural forcing has a seven-day cycle in summer mid-latitudes.

Weekday-high aerosol optical thickness and weekend-high cloud properties are detectable for Houston, but relatively weak (not shown). This is partly because the surface transport over Houston is generally stronger than in New York (cf. Figure 17), which distributes urban aerosols to other regions rapidly. In addition, the larger surface temperature in a sub-tropical city may induce stronger surface-layer and boundary layer mixing, which transports surface aerosols to the free atmosphere faster than mid-latitude cities (Jin et. al. 2004).

### 3.4 Aerosols-clouds-rainfall relationships

For Houston, the interannual cloud optical thickness has minima during summers and maxima during winters, and ranges from 5-25 (Fig. 10a,b). In addition, for water clouds, effective cloud droplet size has an opposite phase to cloud optical thickness. Namely, thick aerosols corresponds to high droplet size and low cloud optical thickness. At first sight, this results seems to be inconsistent with Twomey effect: when there are more aerosols, aerosols serve as CCN and reduce the size of cloud effective radius, and thus increases cloud optical thickness when the liquid water path of the atmosphere layer does not change [Twomey 1977]. However, the Twomey theory is for total column aerosol numbers and assumes that liquid water in clouds does not change. Therefore, Fig. 10 is not suitable to examine the Twomey theory (Platnick, Personal communica-

tion, 2004). Several processes might be responsible for the consistent phase of aerosols- water cloud effective radius observed in Fig. 10: in Houston a significant portion of aerosols are likely transported from the sea (see Figure 17), and sea salt aerosols have large size and may serve as nuclei from some of the cloud droplets that are much larger than average size (Rogers and Yau, 1989). In addition, we notice that more aerosols correspond to smaller ice cloud droplet size (not shown). This suggests that urban aerosols may serve as CCN and reduce cloud base droplets' size due to evaporation (Twomey 1977), and these smaller water droplets are relatively easily lifted to higher altitudes to become ice clouds and thus reduce the averaged ice cloud effective radius (Rosenfeld, talk at 2003 Fall AGU urban session). A third explanation is that, chemical processes may also be responsible for the opposite phase of aerosols-cloud effective radius (Rissman et. al. 2004).

Urban-induced changes to clouds can be detected from the differences of clouds properties over urban and nearby non-urban regions. Figure 11 shows that in summer, water clouds over the Houston region have smaller effective radii than clouds located east and south of Houston, and have larger effective radius than clouds located west and north of Houston. We focus on summer when mesoscale forcing is more dominant than large-scale, strongly forced events (e.g., frontal systems) over urban regions. Urban aerosols are part of the reason for the differences in cloud effective radius. Although the eastern, western, northern, and southern regions of Houston are only displaced  $1^\circ$  ( $\sim 100$  km) from the Houston region, the thermodynamic and kinetic conditions in the environment are quite different as seen from the monthly mean July surface pressure field (not shown). The surface wind is from south to north with high pressure centered to the east (Fig. 17). This configuration transports large-seize sea salt aerosols to aerosols to the eastern and southern regions, which may explain why these re-

gions have large cloud effective radius than the regions to the north and west of Houston. Furthermore, Houston and surrounding regions all have consistent seasonality on cloud effective radius.

Seasonality of cloud top temperature for water clouds is similar to that of aerosol optical thickness, viz., low values in winter months and high values in summer months (Figure 12), for both New York City and Houston. This implies that a low aerosol optical thickness corresponds to cold water clouds and a high aerosol optical thickness corresponds to warm water clouds. A hypothesis is that strong boundary layer mixing transports surface aerosols to high altitude which can further be removed from city through high level winds; this reduces aerosol thickness; meanwhile, stronger vertical mixing moves cloud droplets to colder altitudes causing lower cloud top temperature. On the contrary, modest vertical mixing helps keep aerosols at the surface layer for a high AOT and low cloud top altitude (namely, warm cloud top). In addition, sea salt aerosols may play a role, but currently there are no reliable measurements for examining sea salt aerosols as even the MODIS aerosols coarse fraction has uncertainty that make it unsuitable for detecting the slight signal of sea salt aerosols over land (Kaufman, 20004, personal communication).

Little seasonality is observed for rainfall over Houston and New York City suggesting that rainfall is less directly affected by aerosols than clouds (Figure 13). Around Houston, the TRMM-based accumulated rainfall data illustrated that the maxima monthly mean rainfall occurs in October 2000, May 2001, and September 2002, above 200 mm per month. This is consistent with the transition seasons in this region. In general, New York's rainfall has less month-to-month variation than Houston, with a maximum slightly above 200 mm/month in October 2002. Consequently, effective radius for water clouds is lower in New York City than in Houston (Figure 14a), implying a larger aerosol amount in New

York City than in Houston's, which is consistent with results previously reported in Figures 3 and 6. It seems that with the increase of cloud effective radius for water clouds, accumulated rainfall increases (Figure 14a). More precipitation occurs typically with deep clouds. The effective radius increases with cloud depth. This may be the primary cause of the positive relation in Fig. 14a. In contrast, Figure 14b is for ice clouds, which again show little relationship between effective radius and accumulated rainfall.

Analyzing monthly mean aerosol optical thickness vs. rainfall identifies little one-to-one relationship between aerosol and rainfall in a climatological sense. Figure 15 shows the increase of rainfall corresponds little to change of aerosol optical thickness for New York City and Houston. This implies that there are no inherent relations between aerosols and precipitation amount. *Shepherd and Burian* (2003) reported urban-induced rainfall anomalies over and downwind of Houston. Understanding the mechanism responsible for rainfall anomalies is essential to simulating them in GCMs. The less direct relationship between rainfall and aerosol optical thickness as presented in Figure 15 implies that urban rainfall anomalies is not fully related to aerosol change. This observation is consistent with the recent hypothesis of *Shepherd and Burian* [2003] that dynamic processes like surface convergence and boundary destabilization are more dominant than aerosols for urban-induced convective events.

#### **4. Background Conditions of New York and Houston**

The urban aerosols and their effects vary from one city to another, depending on the city's microstructure (e.g., land use, building density, population density, and living styles), seasons, and prevailing environmental forcing [*Oke*, 1982; *Karl et al.*, 1988, *Jin et al.* 2004]. To understand aerosol and cloud differences between New York and Houston, some knowledge of the human popula-

tion, land cover and land use, and large or regional scale weather systems for these two regions is essential.

Table 1 is the human population, population density, and population change from 1990 to 2000. New York City has a larger population than Houston, and consequently has more intense human activities and anthropogenic aerosol concentration as shown in Figs. 3, 6, and 14a. Specifically, New York has a population of 8,008,278 with population density of 26,401 people per square mile, while Houston has only 1,953,631 people with population density of 3,372 people per square mile (2000 census). This difference might contribute to the factors causing New York to have higher AOT than Houston in the summer months (Fig. 6). Houston population grew faster than New York City from 1990 to 2000: New York increased at 9% and Houston<sup>5</sup> increased at 19%.

Figure 16 shows the difference in the NDVI between July 1981 and July 2000. Both New York City and Houston have experienced significant land cover changes from 1980 to 2000, with corresponding changes in surface greenness, as indicated in NDVI. New York City and its surrounding region seem to have experienced a slightly larger NDVI change over the past 20 years as compared to Houston.

Figure 17 presents the monthly surface wind field based on NCEP re-analysis. In general, surface wind is affected by topography and thus may not exactly follow the pressure system. In July, the Houston area is influenced by high pressure over the sea that advects wind from the ocean to land. During this time period, Houston's surface circulation is dominated by more mesoscale circulations such as sea, bay, and heat island circulations, whereas New York's sur-

---

<sup>5</sup> Nevertheless, Houston is considered to have more oil refinery activity (source: [http://soc.hfac.uh.edu/artman/publish/article\\_49.html](http://soc.hfac.uh.edu/artman/publish/article_49.html)).

face wind comes from the southwest (mostly land cover). This implies that Houston may have larger sea salt aerosols than New York, as ocean sea salt aerosols are transported into the city.

## 5. Final Remarks

Diurnal, seasonal, and interannual variations of aerosols have been studied using satellite, surface, and NCEP reanalysis data. This research reveals that spatial and temporal urban aerosols vary dynamically as a result of various parallel factors, such as human activity, land cover changes, cloud-aerosol interactions, and chemical processes.

Diurnal variations of aerosol are largely affected by weather conditions, but nighttime AOT is, in general, lower than that of daytime. In addition, seasonality of aerosol optical thickness has opposite phase with cloud optical depth and little relationship with rainfall. Weekly cycles of urban aerosols and clouds, in particular, have been observed for the first time in New York. This cycle may be interpreted as a signal of human activities. Nevertheless, this cycle may be less significant in other cities where aerosol transport is strong, which suggests this cycle is weaker than other temporal properties. By all means, the weekly cycle shows a possible human footprint on the local atmosphere-surface system, and is only statistically valid. Furthermore, as a result, aerosols reduce surface insolation. In a normal day of September, the aerosol-induced decrease of surface insolation can be as high as 20-30  $\text{Wm}^{-2}$  (cf. Fig. 2).

Clearly, the dramatic increase and expansion of human activities in the past century has led to significant changes in land use and possible influences on the regional to global climate. Construction of new buildings and roads tends to disturb the natural land (and vegetation) morphology and enhance the surface frictional effects on the atmospheric flows above. The resulting dynamical effects

are to weaken surface flows but to increase the upward turbulent transport of aerosols.

The above results have important implications with respect to modeling urban aerosols, clouds, and rainfall. Specifically, high-resolution satellite observations of aerosols, clouds, and rainfall could be used to update the atmospheric parameters for both numerical weather prediction and global (regional) climate models [Jin and Shepherd 2004]. The global distributions of aerosols and clouds could be utilized to initialize these models or validate the realisms of different model cloud microphysical processes.

**Acknowledgments.** We appreciate two anomalous reviewers for extremely helpful comments on the earlier version of the manuscript. We thank Brent Holben and the AERONET staff for the user-friendly on-line data archive and analysis system in support of AERONET. We also than Zhong Liu for developing an efficient on-line tool for MODIS, NDVI, and TRMM data. Special thanks go to Ming-Dah Chou for helpful discussions on his radiative transfer model. We appreciate the NOAA-CIRES Climate Diagnostics Center for on-line data retrieval and image. This work was funded by the NASA TRMM project under contract number PMM-0022-0069.

## References

- Adler, R. F., G. J. Huffman, D. T. Bolvin, S. Curtis, and E. J. Nelkin, Tropical Rainfall distributions determined using TRMM combined with other satellite and rain gage information, *J. Appl. Meteor.*, 39(12), 2007-2023, 2000.
- Arnfield, A. J., Two decades of urban climate research: A review of turbulence, exchanges of energy and water, and the urban heat island, *International Journal of climatology*, 23, 1-26.
- Cerverny, R. S., and R. C. Balling, Jr., Weekly cycles of air pollutions, precipitation

and tropical cyclones in the coastal NW Atlantic region, *Nature*, 394, 561-563, 1998.

Changnon, S. A. Jr, 1978: Urban effects on severe local storms at St. Louis. *Journal of Applied Meteorology*, 17, 578-592.

Changnon, S. A. 1992: Inadvertent weather modification in urban areas: Lessons for global climate change. *Bulletin American Meteorological Society*, 73, No. 5, 619-627.

Chou, M. D., and M. J. Suarez, A solar radiation parameterization for atmospheric studies, NASA Tech. Memo 104606, Vol. 15, 40 pp., 1999.

Chu, D. A., Y. J. Kaufman, C. Ichoku, L. A. Remer, D. Tanré, B. N. Holben, Validation of MODIS aerosol optical depth retrieval over land, *Geophys. Res. Lett.*, 29(12), doi:10.1029/2001GL013205, 2002.

Chu, D. A., Y. J. Kaufman, G. Zibordi, J. D. Chern, J. Mao, C. Li, and B. N. Holben, Global monitoring of air pollution over land from the Earth Observing System-Terra moderate resolution imaging spectroradiometer (MODIS). *J. of Geophys. Res.* 108(D21), 4461, doi:10.1029/2002JD003179, 2003.

Cleveland, W. S., Graedel, T. E., Kleiner, B., Warner, J. L., Sunday and workday variations in photochemical air pollutants in New Jersey and New York. *Science*, 186, 1037-1038, 1974.

Colarco, P. R., M. R. Schoeberl, B. G. Doddridge, L. T. Marufu, O. Torres, and E. J. Welton, Transport of smoke from Canadian forest fires to the surface near Washington, D. C.: Injection height, entrainment, and optical properties. *J. of Geophys. Res.* 109, D06203, doi: 10.1029/2003JD004248, 2004.

Grimmond, C. S. B. and T. R. Oke, Comparison of heat fluxes from summertime observations in the suburbs of four North American cities. *Journal of Applied Meteorology*, 34, 873-889, 1995.

Dickerson, R. R., S. Kondragunta, G. Stenchikov, K. L. Civerolo, B. G. Doddridge,

- B. N. Holben, The impact of aerosols on solar ultraviolet radiation and photochemical smog. *Science*, 278, 827-830, 1997.
- Duncan, B., R. V. Martin, A. C. Staudt, and R. Yevich, Interannual and seasonal variability of biomass burning emissions constrained by satellite observations. *J. of Geophys. Res.* 108 (D2), 4100, doi:10.1029/2002/JD002378, 2002.
- Eck, T. F., B. N. Holben, J. S. Reid, O. Dubovik, A. Smirnov, N. T. O'Neill, I. Slutsker, and S. Kinne, Wavelength dependence of the optical depth of biomass burning, urban, and desert dust aerosols, *J. Geophys. Res.*, 104(24), 31,333-31,349, 1999.
- Elkus, B., Wilson, K. R., Photochemical air pollution: weekend-weekday differences. *Atmospheric Environment*, 11, 509-515, 1977.
- Ghan, S., R. Easter, J. Hudson, F. Breon, Evaluation of aerosol indirect radiative forcing in MIRAGE, *J. Geophys. Res.*, 106(D6), 5317-5334, 2001.
- Hansen J., M. Sato, and R. Ruedy, Radiative forcing and climate response, *J. Geophys. Res.*, 102, 6831-6864, 1997.
- Holben, B. N., T. F. Eck, I. Slutsker, D. Tanré, J. P. Buis, A. Setzer, E. Vermote, J. A. Reagan, Y. J. Kaufman, T. Nakajima, F. Lavenue, I. Jankowiak, and A. Smirnov, AERONET – A federated instrument network and data archive for aerosol characterization, *Remote Sens. Environ.*, 66, 1-16, 1998.
- Huff, F. A. and J. L. Vogel, 1978: Urban, topographic and diurnal effects on rainfall in the St. Louis region. *Journal of Applied Meteorology*, 17, 565-577.
- IPCC, Intergovernmental Panel on Climate Change, *Climate Change 2001: The Scientific Basis. Contribution of working group 1 to the Third Assessment Report of the Intergovernmental Panel on Climate Change*, edited by J. T. Houghton et. al., 881 pp., Cambridge Univ. Press, New York, 2001.
- Jin, M., R.E. Dickinson, and A. M. Vogelmann, 1997: A Comparison of CCM2/BATS Skin Temperature and Surface-Air Temperature with Satel-

- lite and Surface Observations. *Journal of Climate*, 10, 1505-1524.
- Jin, M. and R. E. Dickinson 2000: A Generalized algorithm for retrieving cloudy sky skin temperature from satellite thermal infrared radiances. *Journal of Geophysical Research*, D22, 27,037-27,047
- Jin, M.: Interpolation of surface radiation temperature measured from polar orbiting satellites to a diurnal cycle. Part 2: Cloudy-pixel Treatment. *Journal of Geophysical Research*, 105, D3, 4061-4076. 2000
- Jin, M. and R. E. Dickinson, 1999: Interpolation of surface radiation temperature measured from polar orbiting satellites to a diurnal cycle. Part 1: Without Clouds. *Journal of Geophysical Research*, 104, 2105-2116, 1999.
- Jin, M. and R. E. Dickinson 2000: A Generalized algorithm for retrieving cloudy sky skin temperature from satellite thermal infrared radiances. *Journal of Geophysical Research*, D22, 27,037-27,047, 2000.
- Jin, M. and R. E. Dickinson: New observational evidence for global warming from satellite, *Geophys. Res. Lett.*, 29(10), 10.1029/2001GL013833, 2002.
- Jin, M., Analyzing Skin Temperature variations from long-term AVHRR *Bulletin of the American Meteorological Society*, 587-600, 2004.
- Jin, M., R. E. Dickinson, and D. Zhang, The footprint of urban climate change through MODIS, To appear on *J. Climate*, 2004.
- Jin, M. and J. M. Shepherd, On including urban landscape in land surface model - How can satellite data help? Submitted to *Bull. AMS*, 2004.
- Karl, T. R., H. F. Diaz, and G. Kukla, Urbanization: Its detection and effect in the United States Climate Record, *J. Climate*, 1, 1099-1123, 1988.
- Kaufman, Y. J., D. Tarré, and O. Boucher, A satellite view of aerosols in the cli-

- mate system, *Nature*, 419, 215-223, 2002.
- Kaufman, Y. J., D. Tanré, L. A. Remer, E. F. Vermote, A. Chu, and B. N. Holben, Operational remote sensing of tropospheric aerosol over land from EOS Moderate Resolution Imaging Spectroradiometer, *J. Geophys. Res.*, 102, 17,051-17,067, 1997.
- Kaufman, Y. J., I. Koren, L. A. Remer, D. Tanre, P. Ginoux, and S. Fan, Dust transport and deposition observed from the Terra-MODIS spacecraft over the Atlantic Ocean, *J. Geophys. Res.*, accepted JGR2003JD004436.
- King, M. D., Y. J. Kaufman, W. P. Menzel, and D. Tanré, Remote sensing of cloud, aerosol, and water vapor properties from the Moderate Resolution Imaging Spectrometer (MODIS), *IEEE. Trans. Geosci. Remote Sens.*, 30, 2-27, 1992.
- King, M. D., L. F. Radke, and P. V. Hobbs: Optical properties of marine stratocumulus clouds modified by ships, *J. Geophys. Res.*, 98, 2729-2739, 1993.
- King, M. D., W. P. Menzel, Y. J. Kaufman, D. Tanré, B. C. Gao, S. Platnick, S. A. Ackerman, L. A. Remer, R. Pincus, and P. A. Hubanks, Cloud and aerosol properties, precipitable water, and profiles of temperature and humidity from MODIS, *IEEE Trans. Geosci. Remote Sens.*, 41, 442-458, 2003.
- Kistler, R., E. Kalnay, W. Collins, S. Saha, G. White, J. Woollen, M. Chelliah, W. Ebisuzaki, M. Kanamitsu, V. Kousky, H. V. D. Dool, R. Jenne, and M. Fiorino, The NCEP-NCAR 50 year reanalysis: Monthly means CD-ROM and documentation, *Bull. Amer. Meteor. Soc.*, 82, 247-267, 2001.
- Lebron, F., A comparison of weekend-weekday ozone and hydrocarbon concentrations in the Baltimore-Washington metropolitan area. *Atmospheric Environment* 9, 861-863, 1975.
- Lelieveld, J, P. J. Crutzen, V. Ramanathan, M. O. Andreae, C. A. M. Brenninkmeijer, T. Campos, G. R. Cass, R. R. Dickerson, H. Fischer, J. A. de Gouw, A.

- Hansel, A. Jefferson, D. Kley, A. T. J. de Laat, S. Lal, M. G. Lawrence, J. M. Lobert, O. L. Mayol-Bracero, A. P. Mitra, T. Novakov, S. J. Oltmans, K. A. Prather, T. Reiner, H. Rodhe, H. A. Scheeren, D. Sikka, and J. Williams, The Indian Ocean Experiment: Widespread air pollution from South and South-east Asia, *Science*, 291, 1031-1036, 2001.
- Linacre, E., and B. Geerts, Estimating the annual mean screen temperature empirically, *Theor. Appl. Climat.*, 71, 43-61, 2002.
- Lonneman, W. A., Kopczynski, S. L., Darley, P.E., Sutterfield, F.D., Hydrocarbon composition of urban air pollution. *Environmental Science and Technology* 8, 229-236, 1974.
- Marr, L. C. and R. A. Harley, Spectral analysis of weekday-weekend differences in ambient ozone, nitrogen oxide, and non-methane hydrocarbon time series in California. *Atmos. Environ.*, 36, 2327-2335, 2002a.
- Marr, L. C., and R. A. Harley, Modeling the effect of weekday-weekend differences in motor vehicle emissions on photochemical air pollution in central California, *Environ. Sci. Technol.*, 36, 4099-4106, 2002b.
- Mace, G. G., Y. Zhang, S. Platnick, M. D. King, P. Minnis, and P. Yang: Evaluation of cirrus cloud properties derived from MODIS radiances using cloud properties derived from ground-based data collected at the ARM SGP site, *J. Appl. Meteor.*, in press, 2004.
- Oke, T. R., The energetic basis of the urban heat island, *Quart. J. Roy. Meteor. Soc.*, 108, 1-24, 1982.
- Smirnov, A., B. N. Holben, T. F. Eck, I. Slutsker, B. Chatenet, and R. T. Pinker, Diurnal variability of aerosol optical depth observed at AERONET (Aerosol Robotic Network) sites, *Geo. Phys. Lett.* 29(23), 2115, doi:10.1029/2002GL016305.
- Platnick, S., M. D. King, S. A. Ackerman, W. P. Menzel, B. A. Baum, J. C. Riédi,

- and R. A. Frey, The MODIS cloud products: Algorithms and examples from Terra, *IEEE Trans. Geosci. Remote Sens.*, 41, 459-473, 2003.
- Ramanathan, V., P. J. Crutzen, J. T. Kiehl, and D. Rosenfeld, Aerosols, climate, and the hydrological cycle, *Science*, 294, 2119-2124, 2001.
- Remer, L. A., and Y. J. Kaufman, Dynamic aerosol model: Urban/industrial aerosol, *J. Geophys. Res.*, 103, 13859-13872, 1998.
- Rissman, T. A., A. Nenes, and J. H. Seinfeld, Chemical Amplification (or Dampening) of the Twomey effect: Conditions derived from droplet activation theory, *J. Atm. Sci.*, 61, 919-930, 2004.
- Rogers, R. R. and M. K. Yau, A short cloud physics (Third edition). Butterworth-Heinemann, pp290.
- Rosenfeld, D., Suppression of rain and snow by urban and industrial air pollution, *Science*, 287, 1793-1796, 2000.
- Schoeberl, M. R., and L. C. Sparling, Trajectory modeling, in Diagnostic Tools in Atmospheric Physics: Enrico Fermi CXVII. Edited by G. Ficocco and G. Visconti, pp289-305, North-Holland, New York.
- Shepherd, J. M., and S. J. Burian, Detection of urban-induced rainfall anomalies in a major coastal city, *Earth Interactions*, 7(4), doi:10.1175/10873562(2003)007, 2003.
- Shepherd, J. M., H. Pierce, and A. J. Negri, Rainfall modification by major urban areas: Observations from spaceborne rain radar on the TRMM satellite, *J. Appl. Meteor.*, 41, 689-701, 2002.
- Shepherd, J.M., and M. Jin, 2004: Linkages between the Urban Environment and Earth's Climate System. *EOS*, 85, 227-228.
- Simpson, J., R. F. Adler, and G. R. North, A proposed Tropical Rainfall Measuring Mission (TRMM) satellite, *Bull. Amer. Meteor. Soc.*, 69, 278-295, 1988.
- Smirnov, A., B. N. Holben, T. F. Eck, O. Dubovik, and I. Slutsker, Cloud screen-

ing and quality control algorithms for the AERONET data base, *Remote Sens. Environ.*, 73, 337-349, 2000.

Stull, R. B., An introduction to boundary layer meteorology. Kluwer Academic Publishers, pp670, 1988.

Thompson, A. M., J. C. Witte, M. T. Freiman, N. A. Phahlane, and G. J. R. Goetzee, 2002, Lusaka, Zambia, during SAFARI-2000: Convergence of local and imported ozone pollution, *Geo. Res. Lett.*, 29 (20), doi:10.1029/2002GL015399.

Twomey, S., The influence of pollution on the shortwave albedo of clouds, *J. Atmos. Sci.*, 34, 1149-1152, 1977.

**Table 1: Population and population density for New York City and Houston.**

City Name	2000 Population	2000 Land Areas (mile <sup>2</sup> )	2000 population /mile <sup>2</sup>	1990 Popu- lation	1990 Land Areas (mile <sup>2</sup> )	1990 popula- tion/ mile <sup>2</sup>	Change in Population
New York City	8,008,278	303.3	26,401	7,322,564	308.9	23,705	9%
Houston	1,953,631	579.5	3,372	1,630,553	539.9	3,020	19%

(Source: US 2000 census from [www.demographia.com/db-2000city50kdens.htm](http://www.demographia.com/db-2000city50kdens.htm))

## FIGURE LEGENDS

- Figure 1. Changes of surface solar radiation induced by urban aerosols for September 1, 2001, based on simulations from a radiative transfer model developed by *Chou and Suarez* [1999]. “diruv” and “difuv” represent direct and diffuse uv radiation, “dirpar” and “difpar” represent direct and diffuse photosynthetically active radiation, and “dirir” and “difir” represent direct and diffuse near-infrared radiation. The “total” represents the total solar radiation, and the values are shown on the right-hand axis in  $\text{Wm}^{-2}$ .
- Figure 2. Monthly average aerosol optical thickness at  $0.56 \mu\text{m}$  for January 2002. These data are produced at a  $1^\circ \times 1^\circ$  latitude-longitude grid worldwide, and are derived from Terra/MODIS measurements.
- Figure 3. Spatial distribution of aerosol optical thickness for the USA. Observations are from Terra/MODIS for (a) June 2000, (b) June 2001, and (c) June 2002.
- Figure 4: Monthly mean diurnal variations of urban aerosol for New York and Houston, respectively. Data are obtained from EPA, (a) monthly mean aerosol quality index for PM<sub>2.5</sub> New York, December 2002; (b) PM<sub>2.5</sub> for December 2002 Houston; and (c) Ozone, for July 2002 Houston. Error bar shown is standard deviation. See text for details.
- Figure 5. Diurnal variation of aerosol optical thickness for New York on July 15 July 2001. Data are based on AERONET GISS station measurements. (a) is back trajectory analysis provided by Thompson (NASA/GSFC) and (b) is AERONET measured aerosol optical thickness. (Sources: Image are produced by <http://www.aeronet.gsfc.gov>)

Figure 6. MODIS-derived monthly mean aerosol optical thickness at  $0.56 \mu\text{m}$  from April 2000 to September 2003 for (a) Houston and (b) New York City.

Figure 7. Averaged weekly distribution of aerosol optical thickness based on AERONET GISS station ( $41^\circ\text{N}$ ,  $74^\circ\text{W}$ ). Data are from August-September 2000, June-September 2001, and June-September 2002. To minimize the transport effect, for each day, only observations within nighttime hours 17:00pm-22:00pm are used to calculate the daily average. And only daily averages smaller than 0.2 are used to analyze the weekly variation. X-axis is day of the week, with "0" as Sunday, "1" as Monday, "2" as Tuesday, "3" as Wednesday, "4" as Thursday, "5" as Friday, and "6" as "Saturday".

Figure 8. Same as Figure 7, weekly variations of aerosol optical thickness for summers of Year 2000, 2001, and 2002 respectively. Due to the data availability, summer 2000 include samples for August-September, summer 2001 for June-September, and summer 2002 for June-September 2002. Data is obtained from AERONET GISS station at New York City ( $41^\circ\text{N}$ ,  $74^\circ\text{W}$ ). To reduce aerosol influence transported from high out-of-city sources, only AOT less than 0.20 were analyzed here.

Figure 9. Weekly distribution of (a) cloud effective radius and (b) cloud integrated water path New York City ( $41^\circ\text{N}$ ,  $74^\circ\text{W}$ ). The data represent the median of the daily averages of June to September 2001 that are then spa-

tially averaged over a 50 km x 50 km region centered on New York City, based on the MODIS 1-km resolution level-2 data.

Figure 10. MODIS-derived relationship between (a) aerosol optical thickness and (b) water cloud optical thickness (solid) and effective radius (dashed) for Houston.

Figure 11. (a) MODIS-derived monthly mean water cloud effective radius for Houston, and east, south, north, and south of Houston. (b) The map for the selected regions of Houston, and east, south, north, and south of Houston. Houston locates between 29°-30°N, and 74° -75°W. All the five regions are 1°×1° box.

Figure 12. Comparison of cloud top temperature of (a) Houston and (b) New York City derived from Terra/MODIS data.

Figure 13. TRMM observed monthly mean rainfall for (a) Houston and (b) New York City from January 2000 to September 2003. The observation product is 3B42, at 1° resolution.

Figure 14. Monthly mean accumulated rainfall vs. cloud effective radius for New York City and Houston (a) for water clouds and (b) for ice clouds. Only summer months (June-September) for 2000-2003 are analyzed.

Figure 15. The scatter plot of MODIS aerosol thickness and TRMM-based accumulated rainfall for Houston and New York City, respectively. The data are monthly mean values for the warm season period (June-September) for 2000, 2001, 2002, and 2003.

Figure 16. NDVI anomalies from 1981 to 2000 for (a) Houston and (b) New York City. Anomalies are calculated using NDVI the specific year minus

NDVI climatology, which is averaged NDVI over 1980-2000.

Figure 17. Monthly mean surface wind for (a) July 2000. (b) July 2001, (c) July 2002, and (d) July 2003. The data are from NCEP/NCAR reanalysis at 2.5 and 2.5 degree.

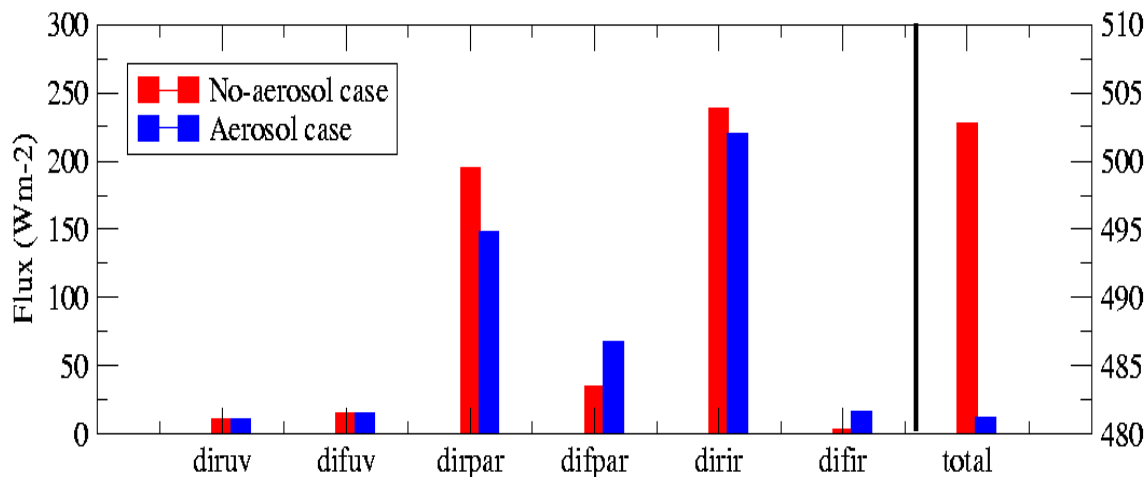


Figure 1. Changes of surface solar radiation induced by urban aerosols for September 1, 2001, based on simulations from a radiative transfer model developed by *Chou and Suarez* [1999]. “diruv” and “difuv” represent direct and diffuse UV radiation, “dirpar” and “difpar” represent direct and diffuse photosynthetically active radiation, and “dirir” and “difir” represent direct and diffuse near-infrared radiation. The “total” represents the total solar radiation, and the values are shown on the right-hand axis in  $\text{Wm}^{-2}$ .

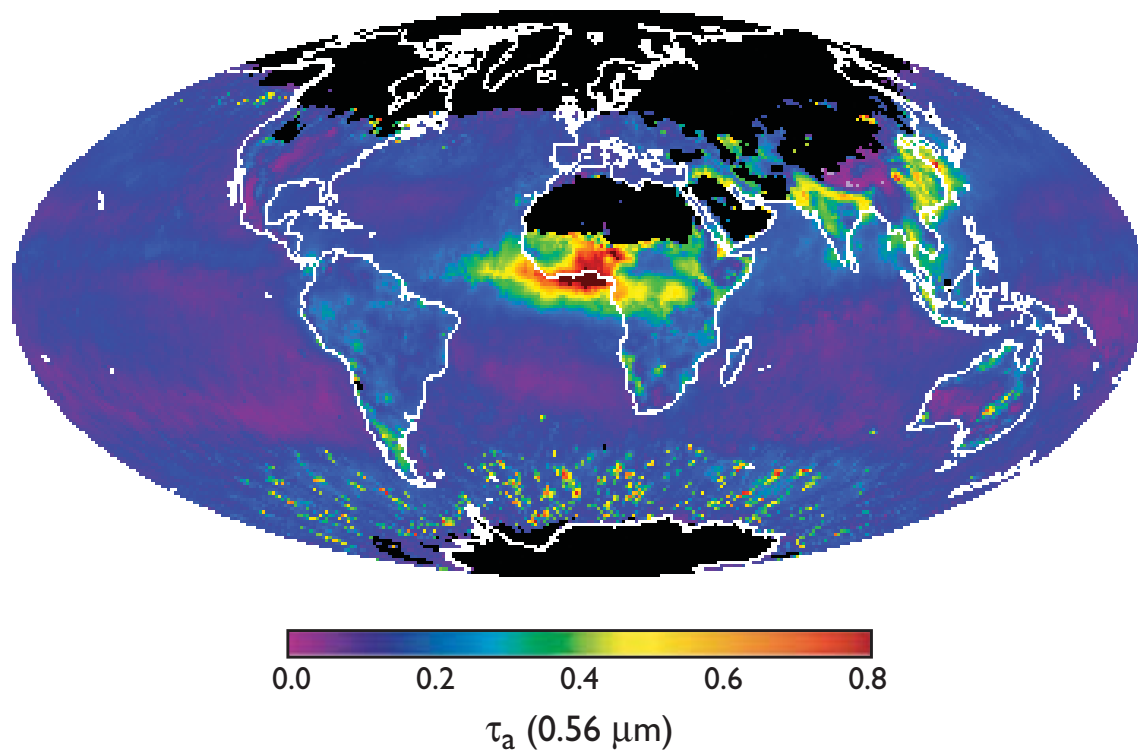
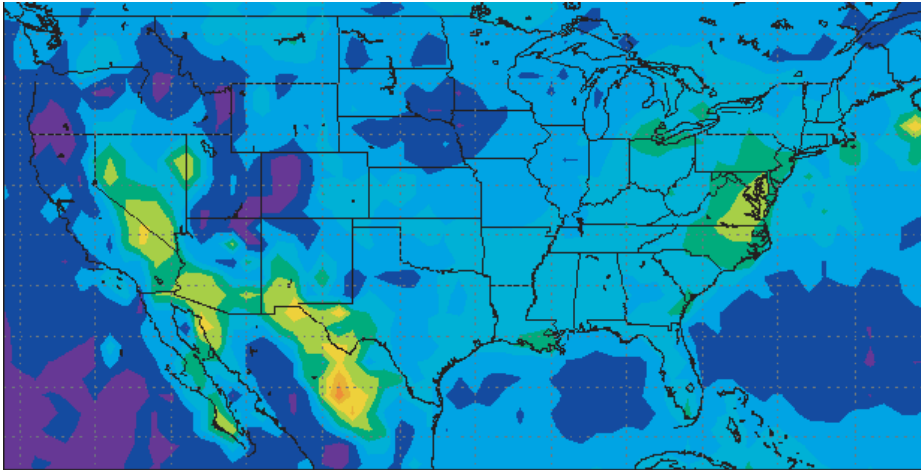
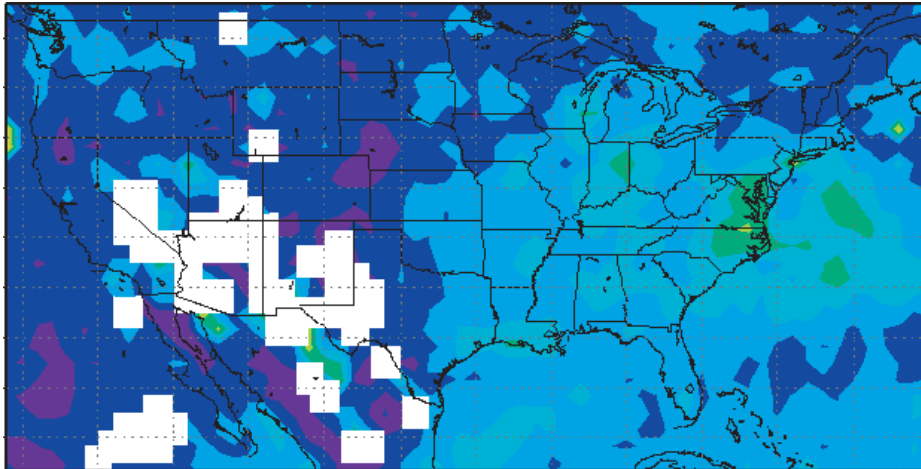


Figure 2. Monthly average aerosol optical thickness at 0.56  $\mu\text{m}$  for January 2002. These data are produced at a  $1^\circ \times 1^\circ$  latitude-longitude grid worldwide, and are derived from Terra/MODIS measurements.

a) June 2000



b) June 2001



c) June 2002

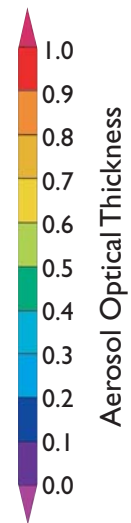
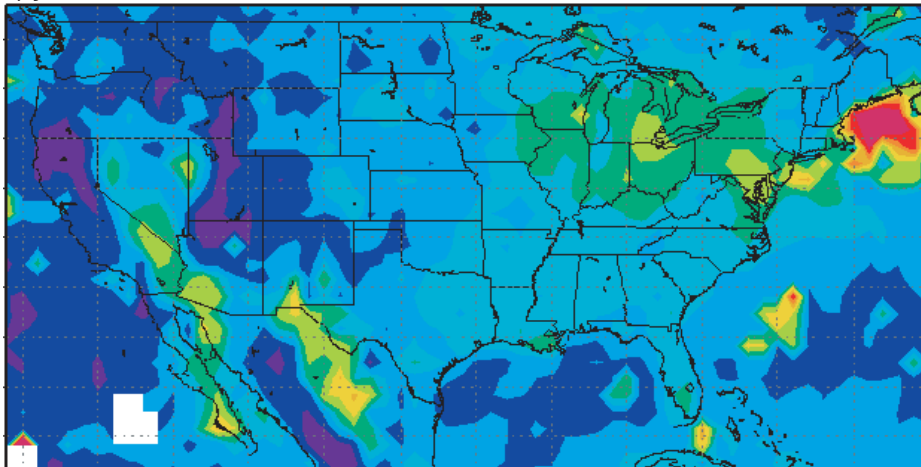


Figure 3: Spatial distribution of aerosol optical thickness for the USA. Observations are from Terra/MODIS for (a) June 2000, (b) June 2001, and (c) June 2002.

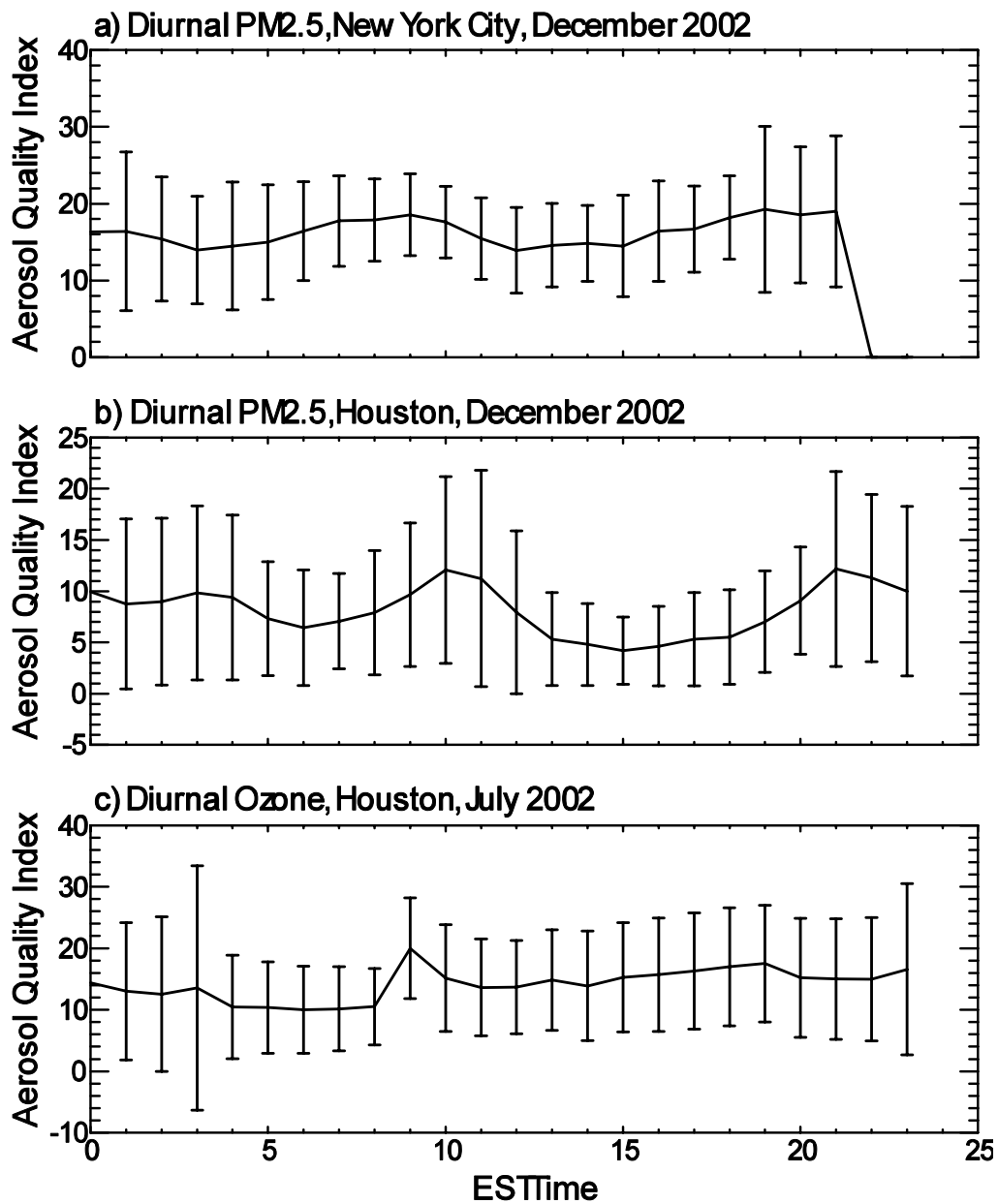


Figure 4: Monthly mean diurnal variations of urban aerosol for New York and Houston, respectively. Data are obtained from EPA, (a) monthly mean aerosol quality index for PM<sub>2.5</sub> New York, December 2002; (b) PM<sub>2.5</sub> for December 2002 Houston; and (c) Ozone, for July 2002 Houston. Error bar shown is standard deviation. See text for details.

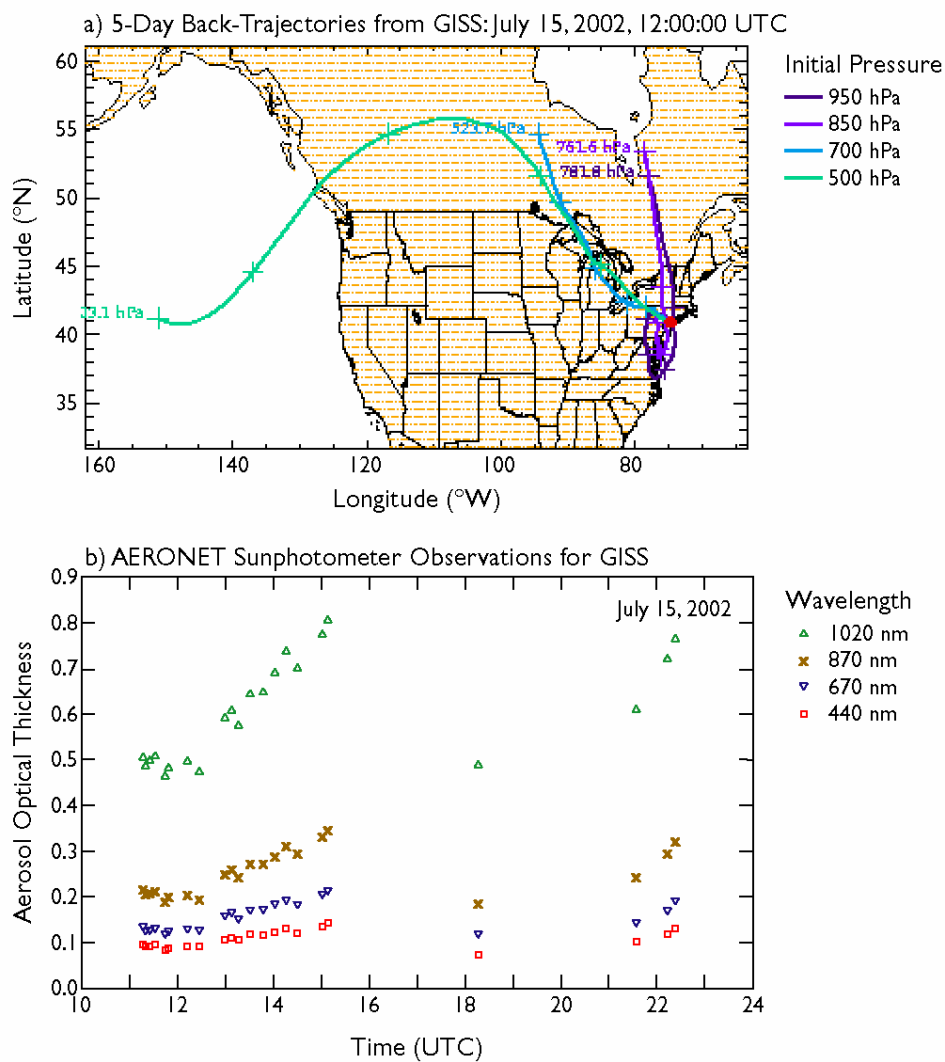


Figure 5. Diurnal variation of aerosol optical thickness for New York on July 15 July 2001. Data are based on AERONET GISS station measurements. (a) is back trajectory analysis provided by Anne Thompson (NASA/GSFC) and (b) is AERONET measured aerosol optical thickness. (Sources: Image are produced by <http://www.aeronet.gsfc.gov>)

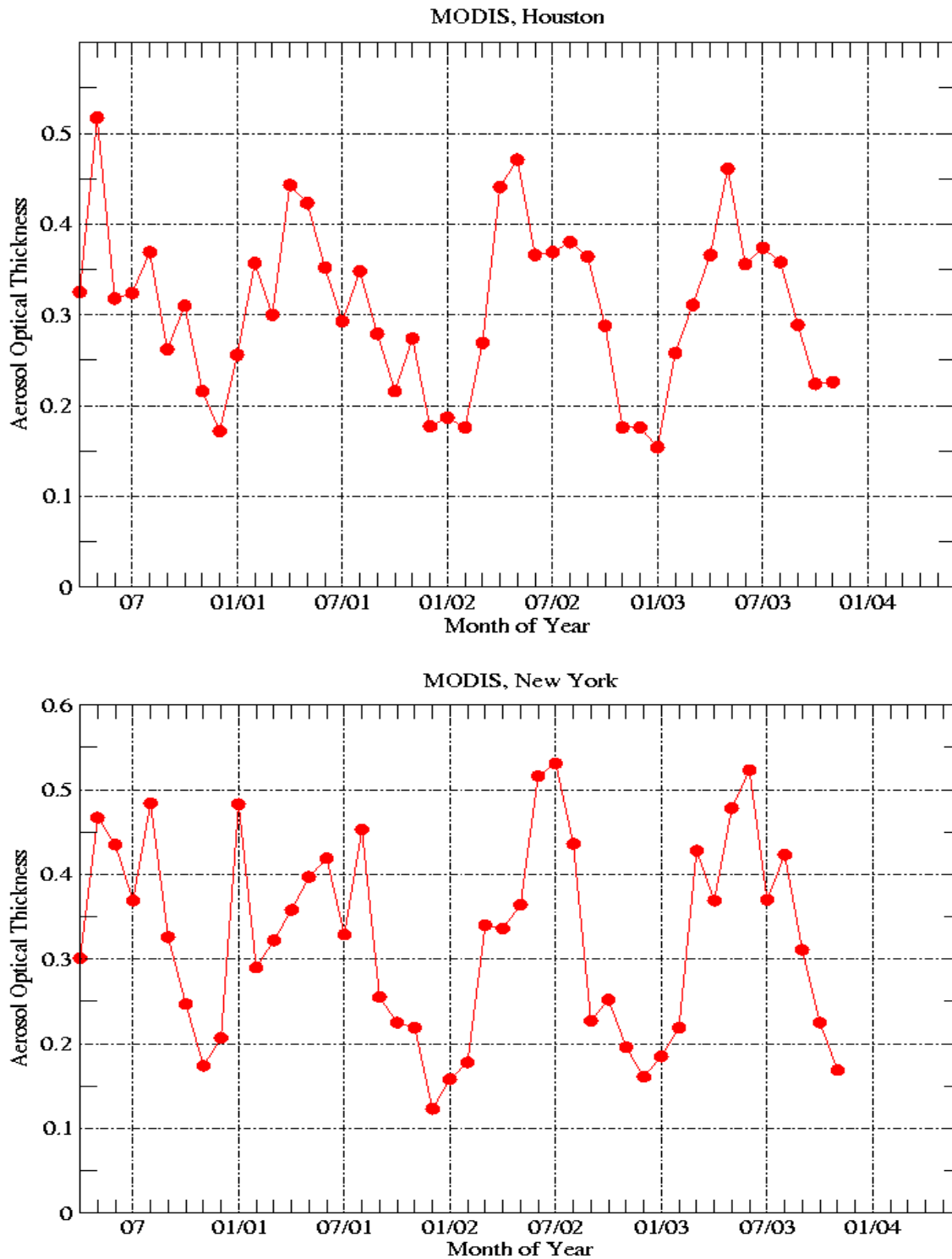


Figure 6. MODIS-derived monthly mean aerosol optical thickness at  $0.56 \mu\text{m}$  from April 2000 to September 2003 for (a) Houston and (b) New York City.

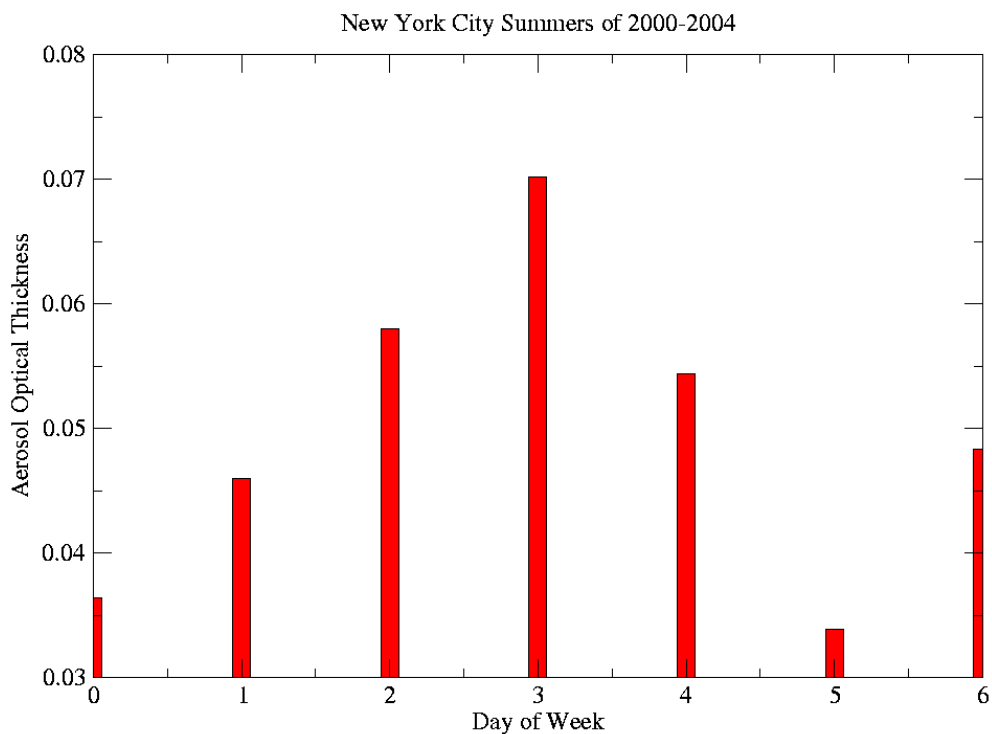


Figure 7. Averaged weekly distribution of aerosol optical thickness based on AERONET GISS station (41°N, 74°W). Data are from August-September 2000, June-September 2001, and June-September 2002. To minimize the transport effect, for each day, only observations within nighttime hours 17:00pm-22:00pm are used to calculate the daily average. And only daily averages smaller than 0.2 are used to analyze the weekly variation. X-axis is day of the week, with “0” as Sunday, “1” as Monday, “2” as Tuesday, “3” as Wednesday, “4” as Thursday, “5” as Friday, and “6” as “Saturday”.

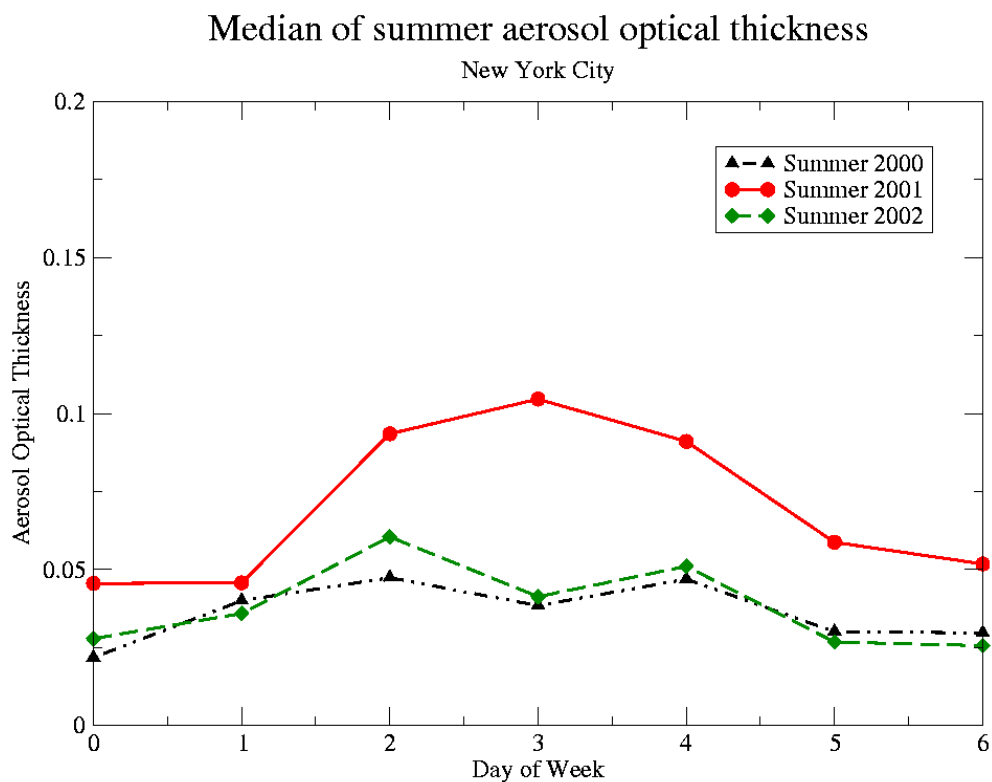


Figure 8. Same as Figure 7, weekly variations of aerosol optical thickness for summers of Year 2000, 2001, and 2002 respectively. Due to the data availability, summer 2000 include samples for August-September, summer 2001 for June-September, and summer 2002 for June-September 2002. Data is obtained from AERONET GISS station at New York City (41°N, 74°W). To reduce aerosol influence transported from high out-of-city sources, only AOT less than 0.20 were analyzed here.

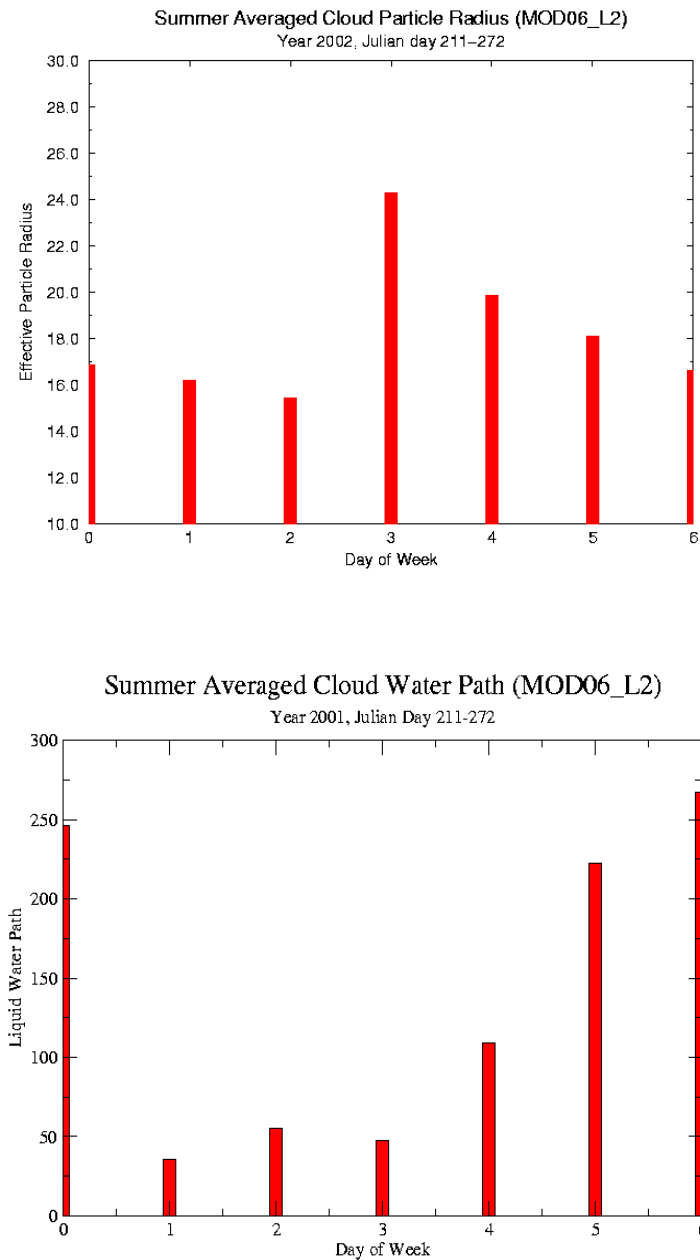


Figure 9. Weekly distribution of (a) cloud effective radius and (b) cloud integrated water path New York City ( $41^{\circ}\text{N}$ ,  $74^{\circ}\text{W}$ ). The data represent the median of the daily averages of June to September 2001 that are then spatially averaged over a  $50\text{ km} \times 50\text{ km}$  region centered on New York City, based on the MODIS 1-km resolution level-2 data.

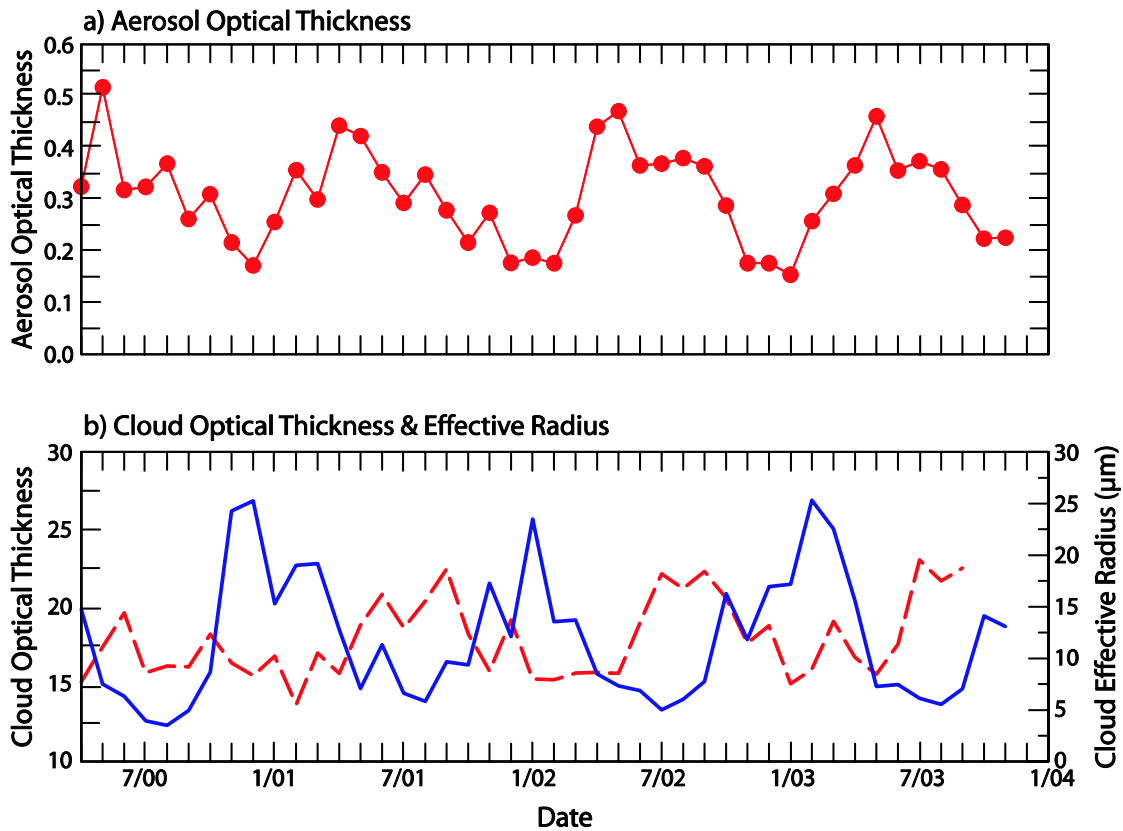


Figure 10. MODIS-derived relationship between (a) aerosol optical thickness at  $0.56\mu\text{m}$  and (b) water cloud optical thickness (solid) and effective radius (dashed) for Houston.

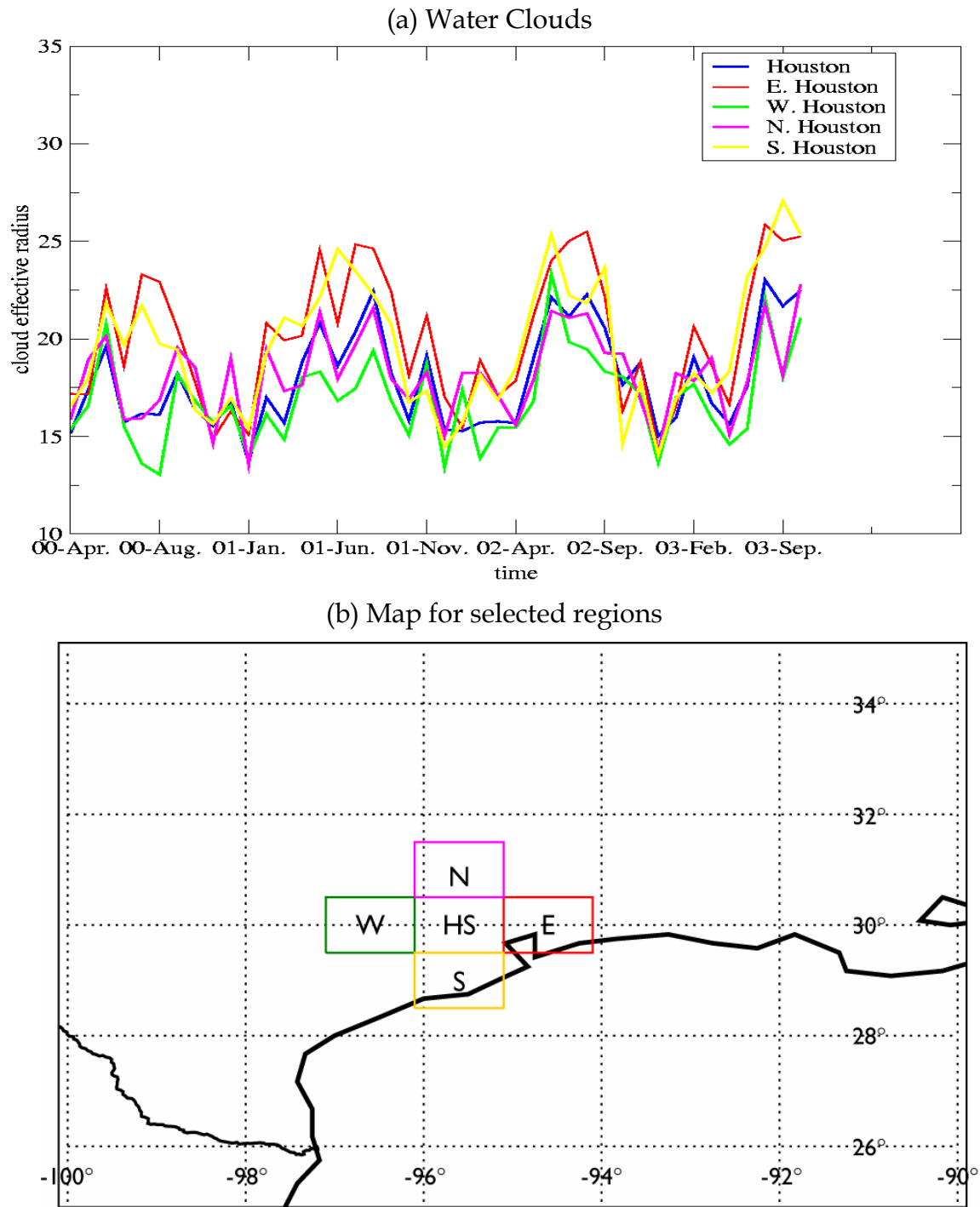


Figure 11. (a) MODIS-derived monthly mean water cloud effective radius for Houston, and east, south, north, and south of Houston. (b) The map for the selected regions of Houston, and east, south, north, and south of Houston. Houston locates between 29°-30°N, and 74° -75°W. All the five regions are 1°×1° box.

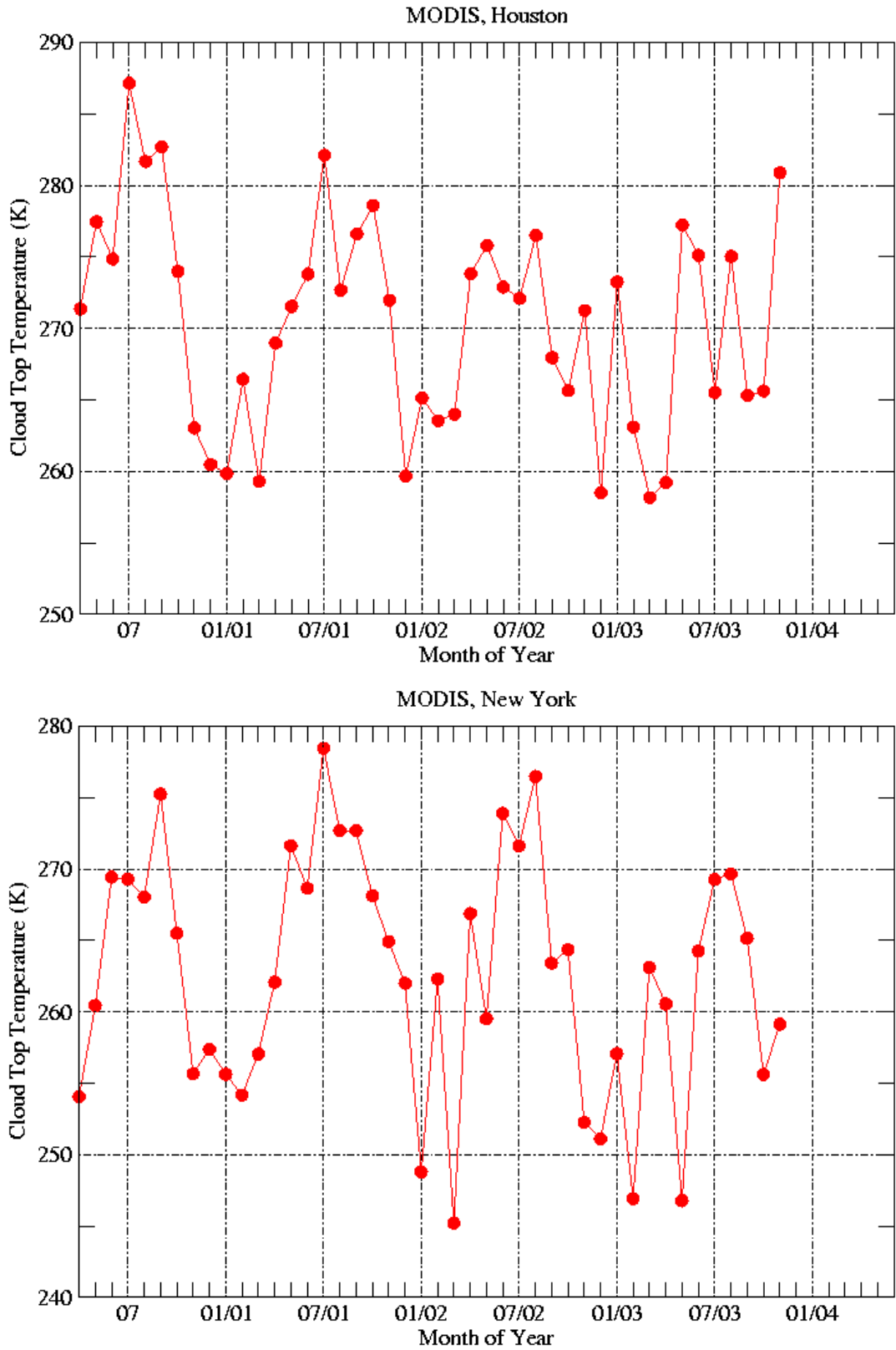


Figure 12. Comparison of cloud top temperature of (a) Houston and (b) New York City derived from Terra/MODIS data.

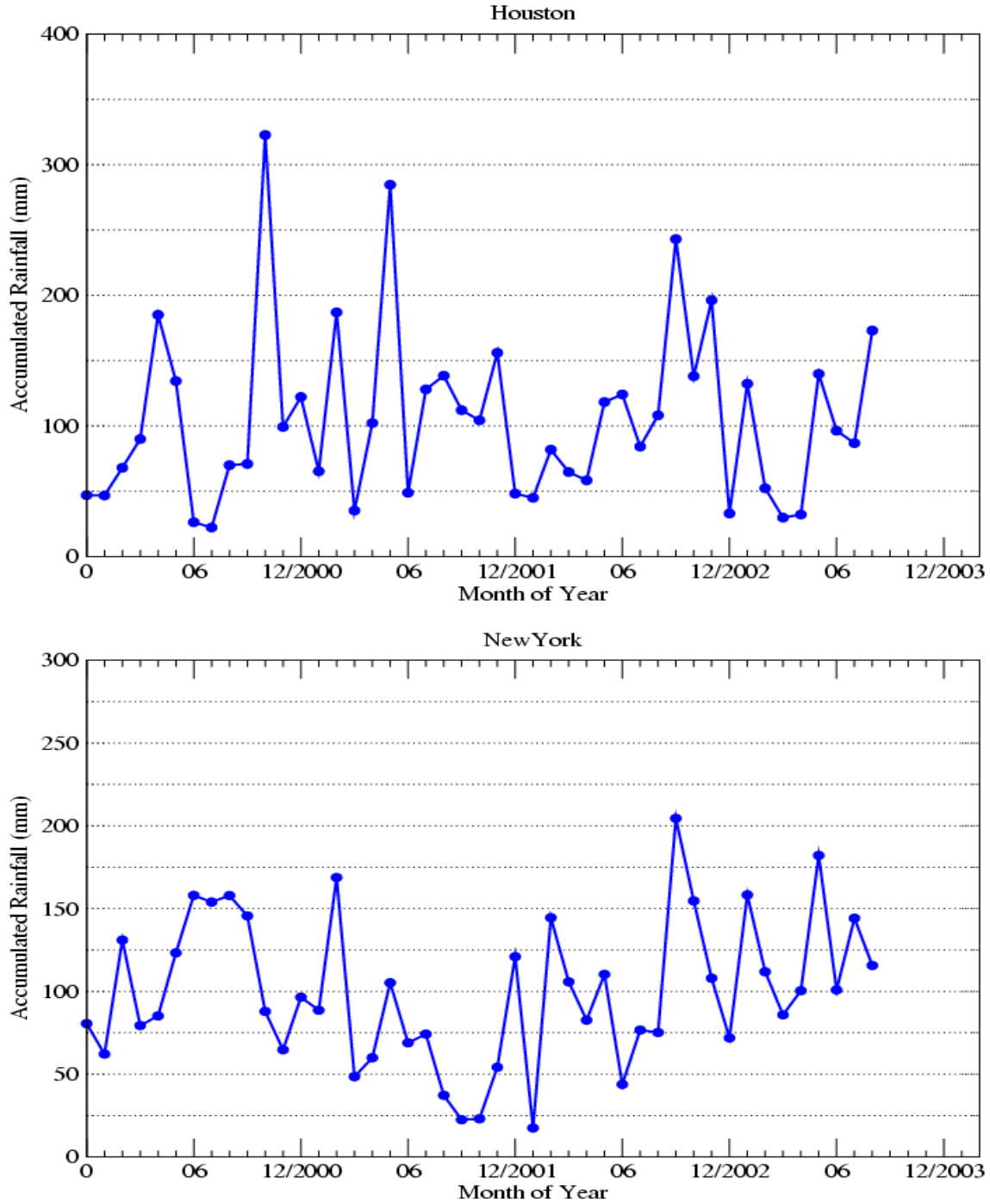


Figure 13. TRMM observed monthly mean rainfall for (a) Houston and (b) New York City from January 2000 to September 2003. The observation product is 3B42, at 1° resolution.

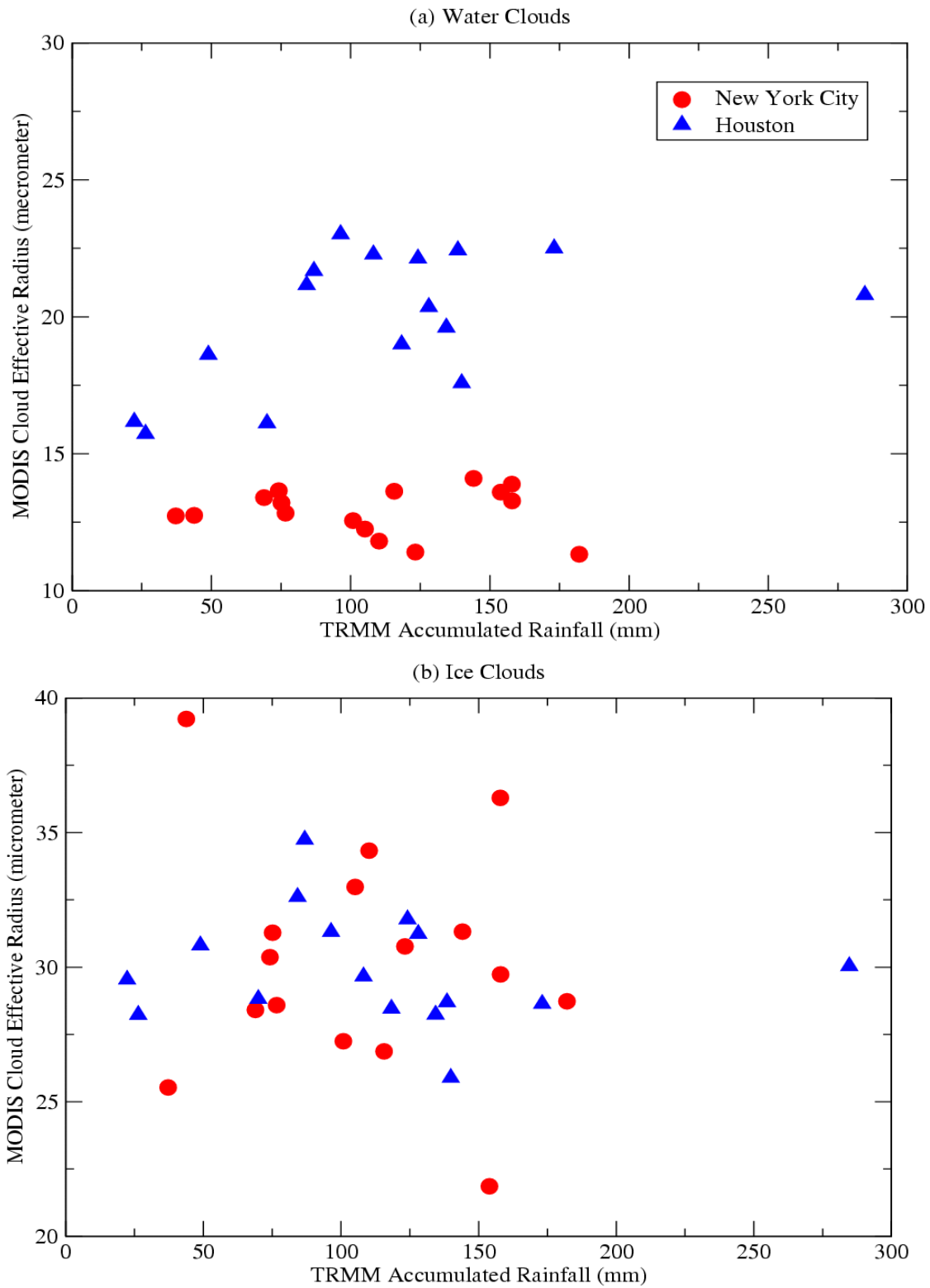


Figure 14. Monthly mean accumulated rainfall vs. cloud effective radius for New York City and Houston (a) for water clouds and (b) for ice clouds. Only summer months (June-September) of 2000-2003 are analyzed.

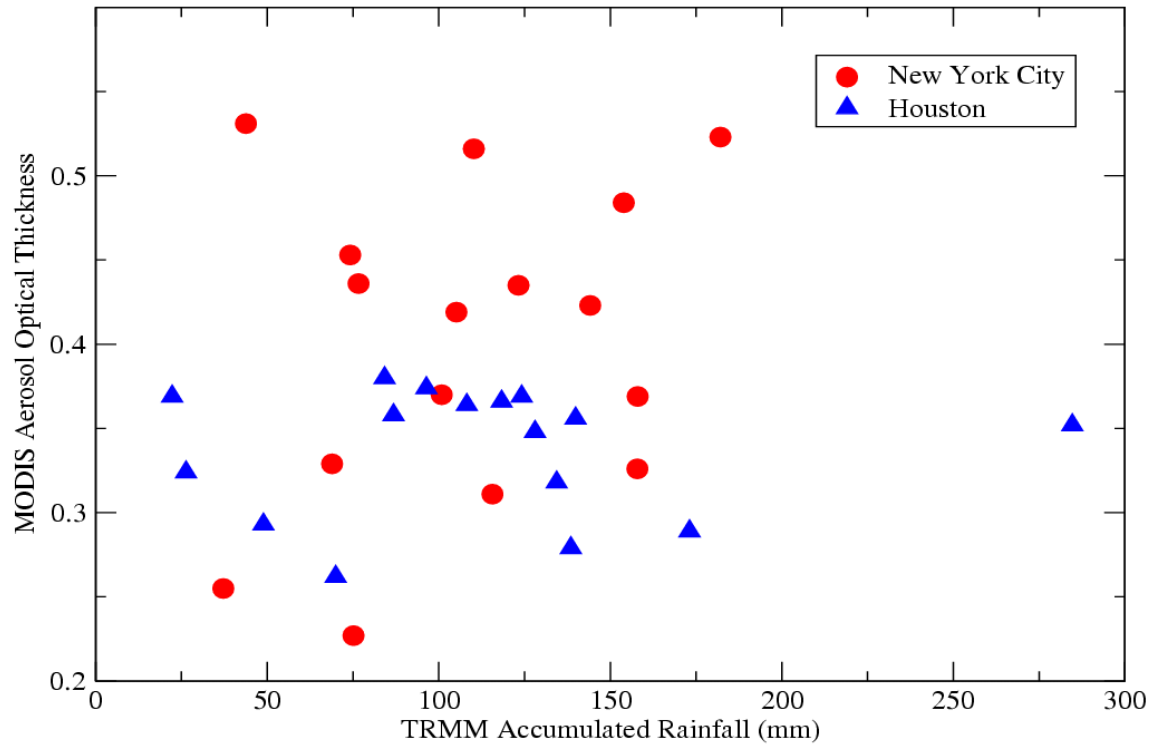


Figure 15. The scatter plot of MODIS aerosol thickness and TRMM-based accumulated rainfall for Houston and New York City, respectively. The data are monthly mean values for the warm season period (June-September) for 2000, 2001, 2002, and 2003.

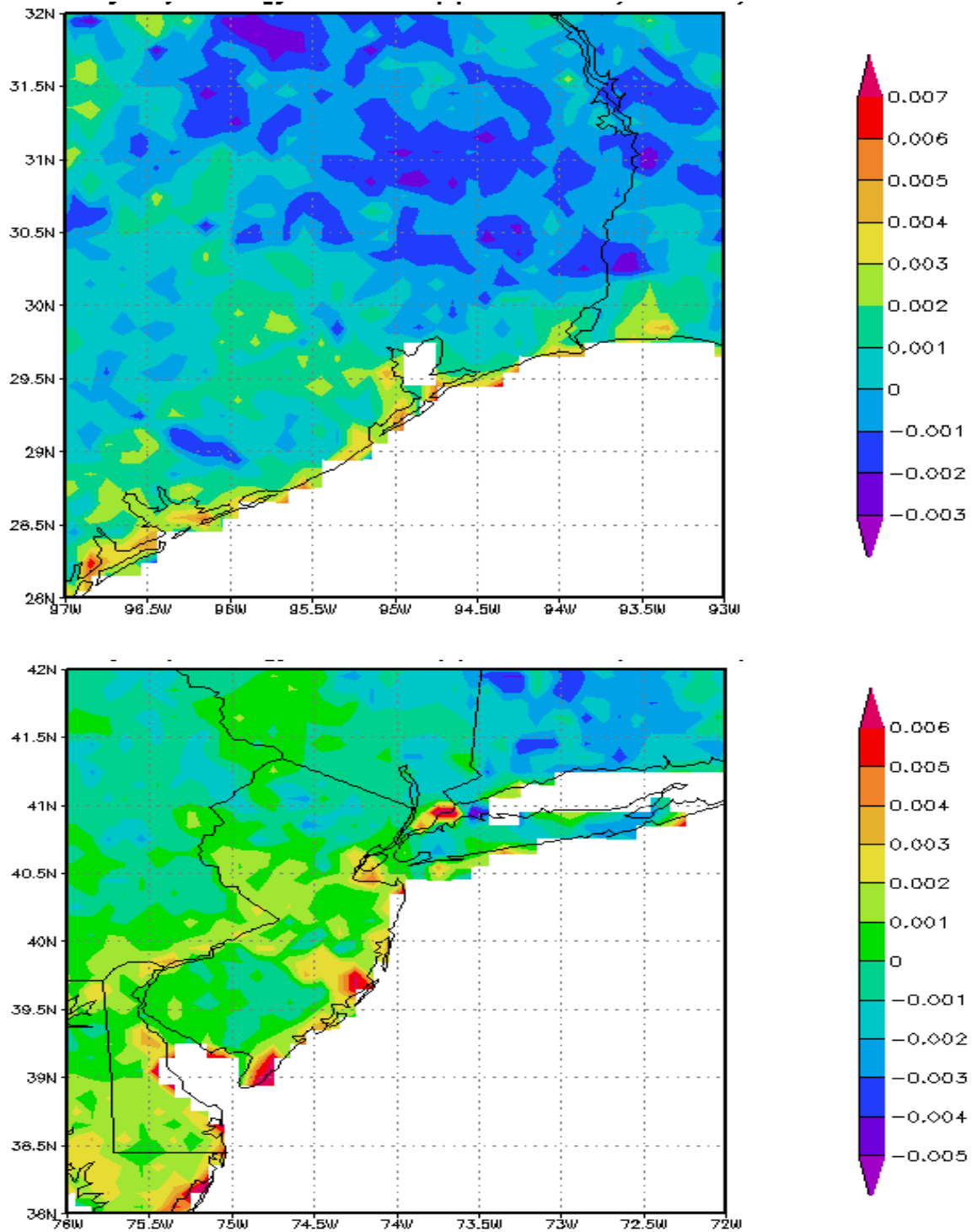


Figure 16. NDVI anomalies from 1981 to 2000 for (a) Houston and (b) New York City. Anomalies are calculated using NDVI the specific year minus NDVI climatology, which is averaged NDVI over 1980-2000.

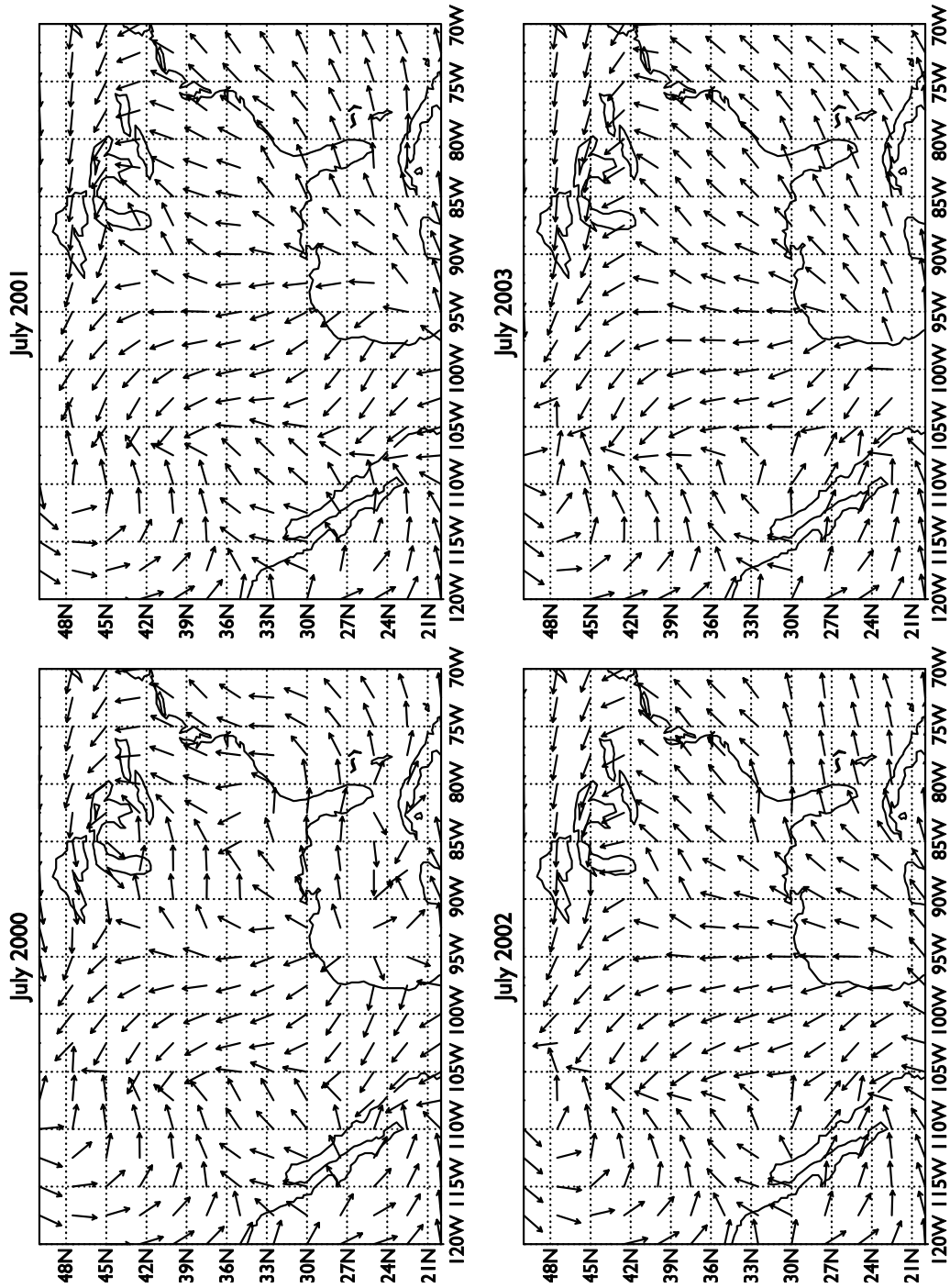


Figure 17. Monthly mean surface wind for (a) July 2000. (b) July 2001, (c) July 2002, and (d) July 2003. The data are from NCEP/NCAR reanalysis at 2.5 and 2.5 degree.